View metadata, citation and similar papers at core.ac.uk

brought to you by CORE

provided by UiS Brage

Universitetet
i Stavanger

FACULTY OF SCIENCE AND TECHNOLOGY

MASTER'S THESIS

Study program/specialization: **MSc in Well Engineering**	**Spring semester, 2019** **Open**
Author: **Muhammad Suleman**	*Suleman* (signature of author)
Program coordinator: External supervisor: **Amare Leulseged** Internal Supervisor: **Professor. Dan Sui**	
Title of master's thesis: **Influence of measured thermophysical parameters of drilling fluids on downhole temperature models**	
Credits: 30	
Keywords: Thermal Conductivity Temperature model Specific heat capacity	Number of pages: 61 + supplemental material/other: …… Stavanger, 29.06.2019

Title page for Master's Thesis
Faculty of Science and Technology

- MASTER THESIS -

Influence of measured thermophysical parameters of drilling fluids on downhole temperature models

Written by:

Muhammad Suleman

Supervise by:

Professor. Dan Sui

Amare Leulseged

Faculty of Science and Technology
Department of Petroleum Engineering

Spring, 2019

ABSTRACT

Predicting downhole circulating temperature is essential for successful drilling operations as bottom hole temperature variations are a major cause of changing effective mud density and mud volume. So, the effort is needed for the development of dynamic modeling capability to simulate the complex downhole temperature environment as Thermal conductivity and specific heat capacity of drilling fluid are an important component in temperature modeling. Despite their importance, very limited data in the literature is available on these parameters. Mostly the values of thermal conductivity and specific heat are estimated using generic models.

An experimental study is performed to measure the thermal conductivity and specific heat capacity of the samples of oil-based mud and water-based mud in the laboratory using the C-Therm TCi thermal conductivity analyzer. Based on the measured values models are generated for thermal conductivity and specific heat capacity of drilling fluid which are then implemented in a simulator on two different wells. The results from these models show the difference of 2.5℃ to 5℃ to in the bottom hole temperature from the generic model for shallow horizontal well and vertical well respectively.

Key Words: Thermal Conductivity, Specific Heat Capacity, Heat transfer, Drilling fluids

ACKNOWLEDGMENTS

This thesis is written and submitted as a fulfillment of the requirements for an MSc degree in Petroleum Engineering with specialization in Well Engineering at the University of Stavanger (UiS), Norway. The work has been carried out in a period between 1st February and 15th June.

All praises are to be for Almighty Allah, the most merciful and beneficent and His last messenger Muhammad (PBUH).

I want to take this opportunity to express my sincere gratitude to my supervisor Professor Dan Sui for her patience, constructive criticism, and showing me the right path throughout the thesis. She was always available to me for guidance and prompt feedback despite her busy schedule.

I am incredibly thankful and indebted to my external supervisor, Amare Leulseged, for sharing his knowledge and expertise on every step. Without his support, this thesis was not possible. It has been a pleasure and an honor!

I would also like to thank Ekaterina Wiktorski for her guidance and sharing her honest and illuminating views related to experimental work.

Lastly, I would like to thank my parents, family, and friends for their constant prayers and support during this journey.

Muhammad Suleman
29.06.2019

This page is intentionally left blank

Table of Contents

List of Figures

List of Tables

CHAPTER 1

INTRODUCTION

1.1 Background

Mud weight is of absolute importance during the drilling operations as it acts as a primary well control barrier and influence other drilling parameters. In offshore, the temperature of the mud pits varies and goes down from zero degree to negative 10°C, and the temperature in the subsurface varies from 60 to 120°C depending on the geothermal gradient. Due to the difference between the external wellbore temperature and fluid temperature, heat transfer occurs. During the process of drilling fluid circulation, the bottom of the well is being cooled and drilling fluid at the bottom is being heated up which causes heat transfer to the upper part of the well [16].

The higher temperature in the wellbore can cause mud weight reduction, so we must consider the temperature variations along the drilling fluid path. There is a significant temperature difference from top to bottom along a wellbore, which can cause localized variations in mud densities. Therefore, it is mandatory that drilling fluid should have appropriate fluid characteristics and heat transfer to have a safe operation especially in cases where the difference between pore pressure and fracture pressure is relatively small [15]. Thermophysical properties like thermal conductivity and specific heat capacity of the drilling fluid affect the heat transfer and play an essential role in the temperature profile of fluids moving in the wellbore. Heat transfer model and many drilling simulators which are being used in the industry incorporate thermal conductivity and specific heat capacity, which are highly dependent on the fluid composition.

Preferable are fluids with high thermal conductivity and high specific heat capacity as they can contribute to lower bottom-hole circulating temperatures which allows the temperature to be equalized faster and hence quicker well stabilization when the well is left static. Also, such fluids are less prone to density reduction at higher bottom hole temperatures [1].

1.2 Purpose

The purpose of the thesis is to review the current knowledge about the estimated values of thermal conductivity and specific heat capacity from different models being used in the heat transfer calculation and then to make a comparison with experimentally measured values and thus based on the difference modify the models. Apply the new values in the simulator 'Drilling Calculator' and do the comparison with the model already being used in the simulator

1.3 Approach

The objectives of the thesis are achieved by:

- Reviewing the literature about temperature model and the models used for calculation of thermal conductivity and specific heat of drilling fluid
- Experimenting in the laboratory to measure the thermal conductivity and specific heat capacity of water-based mud (WBM) and oil-based mud (OBM)
- Input the measured values of the thermal conductivity and specific heat capacity into the drilling calculator and compare it with the model already being used in the simulator

1.4 Structure of the thesis

From this point forward dissertation is organized in the following way:

- In Chapter 2, the current knowledge on thermal conductivity and specific heat capacity and how they are calculated using current models is given
- In Chapter 3, a brief overview of the experimental methodology to measure thermal conductivity and specific heat capacity is given
- In Chapter 4, the results of the experiments as discussed in chapter 3 are presented and analyzed to have a better understanding of thermal properties of the oil-based mud, water-based mud, and their components
- In Chapter 5, simulations are performed on two wells in the drilling calculator and based on the results some conclusions are drawn and recommendations for further work are provided

CHAPTER 2

LITERATURE REVIEW

Moving along the wellbore drilling fluid loses or gains heat to or from its surroundings. However, from the formation to the mud, there is a net transfer of heat as it goes down the well. Mud is still cooler at the bit than the surrounding formation, and it continues to heat up while moving in the annulus towards the surface until it reaches a depth where its temperature equalizes with the formation temperature. After that point, it starts cooling down on its way to surface. Thermal equilibrium can only be achieved under constant circulating conditions [2]. Thermophysical parameters are the properties of the material which affect the heat transfer through that material, and they vary with the temperature, pressure, and composition. These properties include diffusivity, effusivity, heat capacity, thermal conductivity, thermal expansion, etc. The level of influence of these properties on heat exchange depends on different circumstances. In this chapter,

- A brief overview of thermal conductivity is provided in section 2.1
- Specific heat capacity description is presented in section 2.2
- Current models to calculate thermal conductivity and specific heat capacity are given in section 2.3

2.1 Thermal conductivity

Thermal conductivity is an inherent ability of a material to transfer or conduct heat, and it depends on certain properties of a material, specifically its structure and temperature. There is a transfer of heat from an area of high temperature and high molecular energy to an area with a lower temperature and lower molecular energy until thermal equilibrium is reached [3].

Thermal conduction is a result of a direct energy transfer between particles and has nothing to do with macroscopic displacements in the body as in convection. In contrast to heat transfer by radiation, there is no thermal conduction in a vacuum. The phenomenon of thermal conductivity occurs through molecular agitation and contact. Because molecular movement is the basis of thermal conductance, thermal conductivity is primarily influenced by the temperature of a material. Rate of heat transfer at elevated temperatures is higher because of

the quicker movement of molecules. Hence, with the increase or decrease in temperature thermal conductivity of the same sample changes significantly [17].

"Thermal conductivity is defined as the quantity of heat (Q) transmitted through a unit thickness (L) in a direction normal to a surface of unit area (A) due to a unit temperature gradient (ΔT) under steady state conditions and when the heat transfer is dependent only on the temperature gradient" [4]. It can be calculated using the following equation:

$$k = \frac{Q*L}{A(\Delta T)} \text{ [W/mK]} \quad (2.1)$$

Thermal conductivity of solids and especially metals are higher, but it depends on the conductivity of the material. Thermal conductivity of liquids comes after and under normal conditions is much lower than that of metals and ranges from 0.1 to 0.6 W/mK. The lowest thermal conductivity can be observed in gases, which range from 0.006 to 0.1 W/mK [12].

Table_2.1

Values of the coefficient of thermal conductivity for various substances at atmospheric pressure and moderate temperatures [13]

Cotton	0.04
Cotton wool	0.029
Diamond	1000
Engine Oil	0.15
Graphite	168
Ground or soil, dry area	0.5
Ground or soil, moist area	
Polyethylene - low density	0.33
Polypropylene, PP	0.1 - 0.22
Porcelain	1.5
Sulfur, crystal	0.2
Uranium dioxide	8.8
Water	0.58

Thermal conductivity of generic water-based mud is around $0.575\ W/m.k$ [5] and that of generic oil-based mud is around $0.275\ W/m.k$ [6]. Use of certain type of drilling fluid in the drilling operation is determined by its thermal conductivity. For example, in high pressure and high temperature wells where the heat transfer demands on the drilling fluid is much greater, we need a mud which is thermally stable and have high thermal conductivity. [7]

2.2 Specific heat capacity

Specific heat is an intensive property which describes how much heat must be added to a unit of mass of a given substance to raise its temperature by 1°C. It is commonly measured in J/(kg*K). Heat capacity is referred to as an extensive property that describes how much heat energy it will take to raise the temperature of the whole system. But to measure the heat capacity of each unit of matter is inconvenient so we need a measurement of an intensive property that depends only on the type and phase of a substance and can't change with the size of system or amount of material present in the body. This quantity is termed as the specific heat capacity, which is the heat capacity per unit mass of material. [8]

The amount of heat needed for a temperature change depends on the mass of the system, phase of substance, and the magnitude of temperature change. As the kinetic energy of an atom is directly proportional to the absolute temperature and the internal energy of a system is proportional to the absolute temperature and the number of atoms and since the transferred heat is equal to the change in the internal energy, the heat is proportional to the mass of the substance and the temperature change. The amount of heat transferred also depends on the type of substance as heat required to raise the temperature by 1 degree for alcohol is less than for water. It also depends on the phase (gas, liquid, or solid). The quantitative relationship between heat transfer and temperature change contains all three factors [19]:

$$Q = mc\Delta T \tag{2.2}$$

where,
Q = symbol for heat transfer
m = mass of a substance
c = symbol for specific heat capacity and depends on material and phase
ΔT= temperature change

Specific heat also depends on temperature. For liquids and solids, the volume and temperature dependence of the specific heat capacity is weak, but this is not true for gases. The specific heat of water-based mud is generally higher than that of oil-based mud, which means that it takes more heat to raise the temperature of water-based mud then that of oil-

based mud. Thus, specific heat capacity is also one of the important factors in the designing of drilling fluid [18].

2.3 Heat transfer model

To predict the transient thermal behavior of the well during drilling, the knowledge about the temperature distribution of the circulating drilling fluids, the wellbore, and the surrounding formation is required. Many variables are changing, so it is difficult to determine the transient temperature. To do accurate modeling, extensive knowledge of the thermal and transport properties of all the materials and especially drilling fluid is required. Generally, the formation and drill string properties are well characterized. However, the variation with temperature or composition of the transport and thermophysical properties of drilling fluids and cement is less known. The function of drilling fluid circulation is to cool and lubricate the bit, to transport the cuttings to the surface, and to control subsurface pressures, among other, fluid circulation also produces a cooling effect of the surrounding formation and thus acts as a tool for predicting wellbore temperatures [20].

Several models have been developed to study the heat transfer during circulation. Holmes and Swift obtained a steady state solution to the wellbore heat transfer equations which can not be applied to transiet behavior [22]. Raymond develop a method of predicting temperatutre distributions for transient as well as pseudo steady state conditions [23]. Marshall and Bentsen in 1982 provides a computer based model based on the Raymond model of wellbore transient heat transfer which is more accurate and efficient. Fluid temperature is dependent upon different thermal processes. Fluid with known temperature enters the drillpipe and its change in temperature is determined by rate of vertical thermal convection, radial rate of convective heat transfer between the fluid, the pipe wall and annulus, vertical and radial heat conduction. Just like heat generated due to frictional forces and rotational energy of drill string and the drill bit, time of circulation has also an important effect on temperature of fluid because of transient heat transfer [24]. The final form of energy conservation as a result of heat transfer can be written as:

$$\frac{\partial}{\partial t}[\rho_m(t,s)H(t,s)] - \nabla\big[Q_f(t,s) + Q_c(t,s)\big] - Q_s(t,s) = 0 \qquad (2.3)$$

where H is the enthalpy per unit mass, Q_f is the convective term, Q_c is conductive term and Q_s is mechanically generated heat.

The forced convective term can be expressed as

$$Q_f = \rho_m(t,s)H(t,s)v_m(t,s) \tag{2.4}$$

The conductive and natural convective term does not have a general expression. In case of purely isotropic material, we can use:

$$Q_c = k(t,s)\nabla T(t,s) \tag{2.5}$$

where k is the thermal conductivity and T is the temperature. [9]

2.3.1 *Thermal conductivity calculation*

Thermal conductivity calculation for the drilling fluid is not popular, and very little work is done for estimating the thermal conductivity of liquid mixtures and minimal data is available in the literature.

Tsederberg method

The primary and simple method is given by Tsederberg to calculate the thermal conductivity of the liquid mixture and is shown by the equation below [25]:

$$k_m = k_{c1}m_1 + k_{c2}m_2 \tag{2.6}$$

For n number of components, it can be written as:

$$k_m = \sum_{i=1}^{n} k_{ci}\, m_i \quad [\mathrm{W/mK}] \tag{2.7}$$

where,

k_m = thermal conductivity of the mixture

k_{c1}, k_{c2}= thermal conductivity of components

m_1, m_2= mass fractions of components

Jamieson et al. Correlation

For binary mixtures in 1975, Jamieson et al. suggested the following relation which has been extensively tested on many types of mixtures to calculate thermal conductivity [26]:

$$k_m = k_{c1}m_1 + k_{c2}m_2 - \alpha(kc_2 - kc_1)[1 - m_2^{\frac{1}{2}}]m_2 \quad [\mathrm{W/mK}] \tag{2.8}$$

Where components are so selected that $kc_2 > k_{c1}$ and α is an adjustable parameter that is set equal to unity if mixture data is available for regression purpose.

Maxwell model

Maxwell in 1872 described the solution to calculate the effective thermal conductivity of suspension of the homogeneous solid-liquid mixture with an assumption that solid particles are spherical in shape and their concentration in the mixture is small. Maxwell's expression is as follows [26]:

$$\frac{k_m}{k_c} = \frac{{}^{k_d}/_{k_c} + 2 - 2V_d(1 - {}^{k_d}/_{k_c})}{{}^{k_d}/_{k_c} + 2 + V_d(1 - {}^{k_d}/_{k_c})}) \tag{2.9}$$

where,

k_d = thermal conductivity of discontinuous phase (solid particles)

k_c = thermal conductivity of continuous phase

V_d = The volume fraction of discontinuous phase

Rayleigh model

Generally, in the drilling fluid, the particles are not uniform; also the concentration of particles is quite a lot. Rayleigh modified the Maxwell model for a higher concentration of particles, which is expressed by the equation below [13]:

$$\frac{k_m}{k_c} = 1 - \frac{3V_d}{\left(\frac{2 + {}^{k_d}/_{k_c}}{1 - {}^{k_d}/_{k_c}}\right) + V_d - \left(\frac{1 - {}^{k_d}/_{k_c}}{\frac{4}{3} + {}^{k_d}/_{k_c}}\right) * aV_d^{\frac{10}{3}}} \tag{2.10}$$

where,

a = 1.31 for simple cubic array

a = .129 for body centered cubic

a = .0752 for face centered cubic

Churchill model

The variance between Maxwell 's result and Rayleigh's result become more significant with increasing V_d. At V_d = 0.5236, the spherical particles in the cubic lattice are in point contact, and for ${}^{k_d}/_{k_c} \to \infty$ the k_m should approach ∞ at V_d = 0.5236 but these conditions are not met by Rayleigh's expression. Therefore, by considering higher order terms in the series expansion for the potential in the continuous phase. Rayleigh's result is being modified by Meredith and Tobias, 1960, which provides an analytical expression which agrees with the data in a critical range near V_d = 0.5236. The final expression of the effective thermal conductivity of the drilling mud is given as [21]:

$$k_m = k_c \frac{\frac{2+{}^{k_d}/_{k_c}}{1-{}^{k_d}/_{k_c}} - 2V_d + 0.409\frac{6+3{}^{k_d}/_{k_c}}{4+3{}^{k_d}/_{k_c}} V_d^{\frac{7}{3}} - 2.133\frac{3-3{}^{k_d}/_{k_c}}{4+3{}^{k_d}/_{k_c}} V_d^{\frac{10}{3}}}{\frac{2+{}^{k_d}/_{k_c}}{1-{}^{k_d}/_{k_c}} + V_d + 0.409\frac{6+3{}^{k_d}/_{k_c}}{4+3{}^{k_d}/_{k_c}} V_d^{\frac{7}{3}} - 0.906\frac{3-3{}^{k_d}/_{k_c}}{4+3{}^{k_d}/_{k_c}} V_d^{\frac{10}{3}}} \text{ [W/mK]} \tag{2.11}$$

And

$$k_c = \sum_{i \in \Theta} m_i \, k_{ci} \tag{2.12}$$

where Θ is set of indices for liquid components and m_i is the mass fraction of ith component relative to the mass of liquid mix and kc_i is the thermal conductivity of the ith component of liquid.

The liquid phase, which is the background continuous medium, can be a solution of different fluids having different thermal conductivity values. Churchill formula takes one component at a time and uses the resulting thermal conductivity as the a thermal conductivity of the background medium when adding the next component. [9]

2.3.2 *Specific heat capacity calculation*

Specific heat capacity of each component in a multicomponent system is calculated theoretically by the weighted averages in terms of mass fraction and is given as [9]:

$$C_{p_m} = \sum_{i \in \Omega} m_i \, C_{p_i}, \qquad with \; \forall i \; \in \Omega, \qquad m_i = \frac{f_i \rho_i}{\rho_m} \tag{2.13}$$

where,

C_{p_m} = specific heat of drilling mud

$m_i, i \in \Omega$ = are the mass fractions of the components

$C_{p_i}, i \in \Omega$ = are specific heat capacities of each component

Ω = set of indices representing each component

Here the mass fractions can be derived from the volume fractions as we know the density of the components. Whereas, the specific heat capacity of each component is not known, which results in big uncertainty in the estimated specific heat capacity value of the mix. So, a better approach is to measure the specific heat capacity values in the lab to verify the estimation.

CHAPTER 3

METHODOLOGY

Thermal conductivity of the drilling fluid and the base components is measured experimentally using C-Therm's TCi thermal conductivity analyzer and Tenney Junior Test Chamber. Specific heat capacity is calculated by measuring the density of the components experimentally using Anton Paar density meter. The detailed experimental procedure and description of the equipment will be discussed in this chapter.

3.1 Thermal conductivity measurement

Thermal conductivity and thermal effusivity are calculated directly using the C-Therm TCi thermal conductivity analyzer by comparing the sensor response to the factory calibration. There is no need for special sample preparation, and the analyzer has been factory calibrated for various material groups. Usually, the system measures thermal conductivity in Watts per meter-kelvin (W/mK) but unit systems can be changed in the system if desired. The system has testing capability across a temperature range of -50 to 200°C and the pressure range up to 120 psi. Testing time is usually less than a minute. The instrument is susceptible, so stable environmental conditions need to be provided to optimize the performance. The material testing summary showing the required power level, temperature range, and required minimum thickness of the sample as provided by the manual of the equipment is shown in the table given below:

Table_3.1 Material testing summary

Material Type	Minimum Thickness	Power Level	Temperature Range (°C)	Sample Setup & Preparation
Liquids	1 mm	37	-50 to 192	Use Small Volume Test Kit
Powders	1 mm	37	-50 to 192	Use Compression Test Accessory or Small Volume Test Kit

3.1.1 *Experimental setup*

The equipment, as shown in the figure below consists of a controller with the sensor, thermal chamber, a laptop with the C-Therm TCi software installed, and cables.

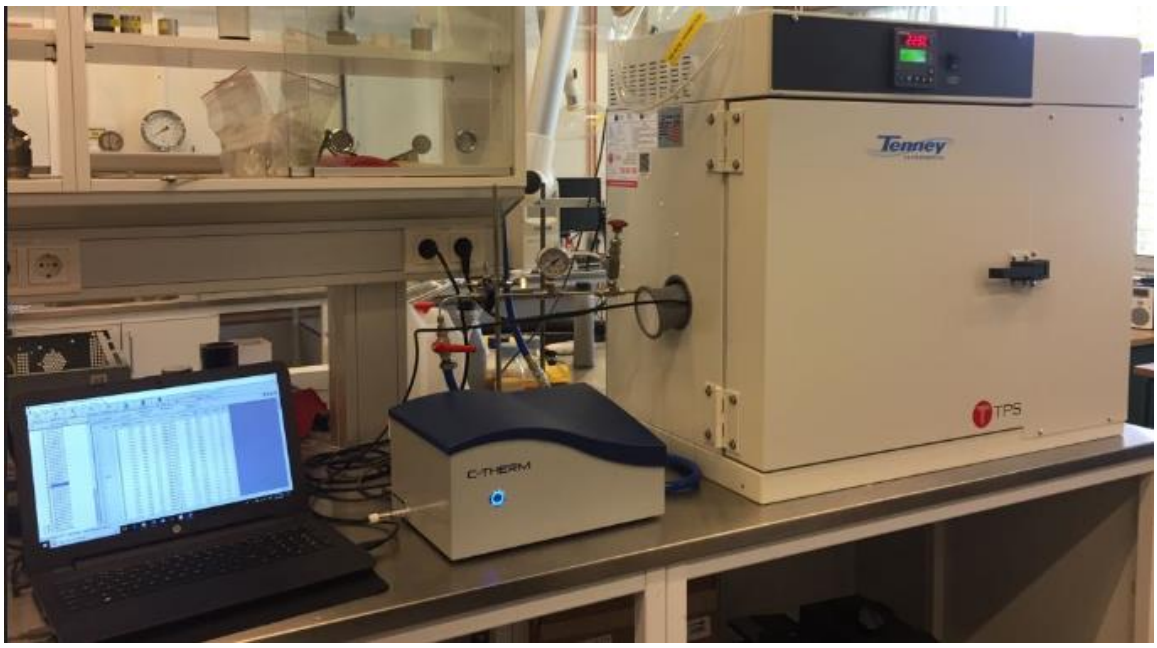

Figure_3.1 Setup showing laptop, C-Therm controller in the center and Tenney thermal chamber

The description of each of them as per the manual is given below:

C-Therm TCi controller with sensor

The pre-calibrated sensor is attached with the controller and placed inside the thermal chamber to avoid environmental fluctuations where calibrations are stored in the database and the sensor chip. The thermal conductivity of the samples is measured by the C-Therm TCi thermal conductivity analyzer using the patent of Modified Transient Plane Source (MTPS) method. This method involves a one-sided heat reflecting sensor embedded with a heating element and is encircled by a guard ring. The heat generated is transferred in one directional plane to the sample when the current is being applied to the sensor and the guard ring instantaneously. Voltage drop is attuned to the temperature change. Thermal conductivity is inversely proportional to the rate of increase in temperature, as seen in the graph. Thus, if the sample is a poor conductor or in other words have very low thermal conductivity, then the slope of the temperature rise will be steep as compared to the sample with high thermal conductivity. During the initial 0.3 seconds when the sample is establishing contact the graph

shows a non-linear curve, and after that, until 0.8 seconds a linear curve is obtained because the heat has now been transferred into the sample.

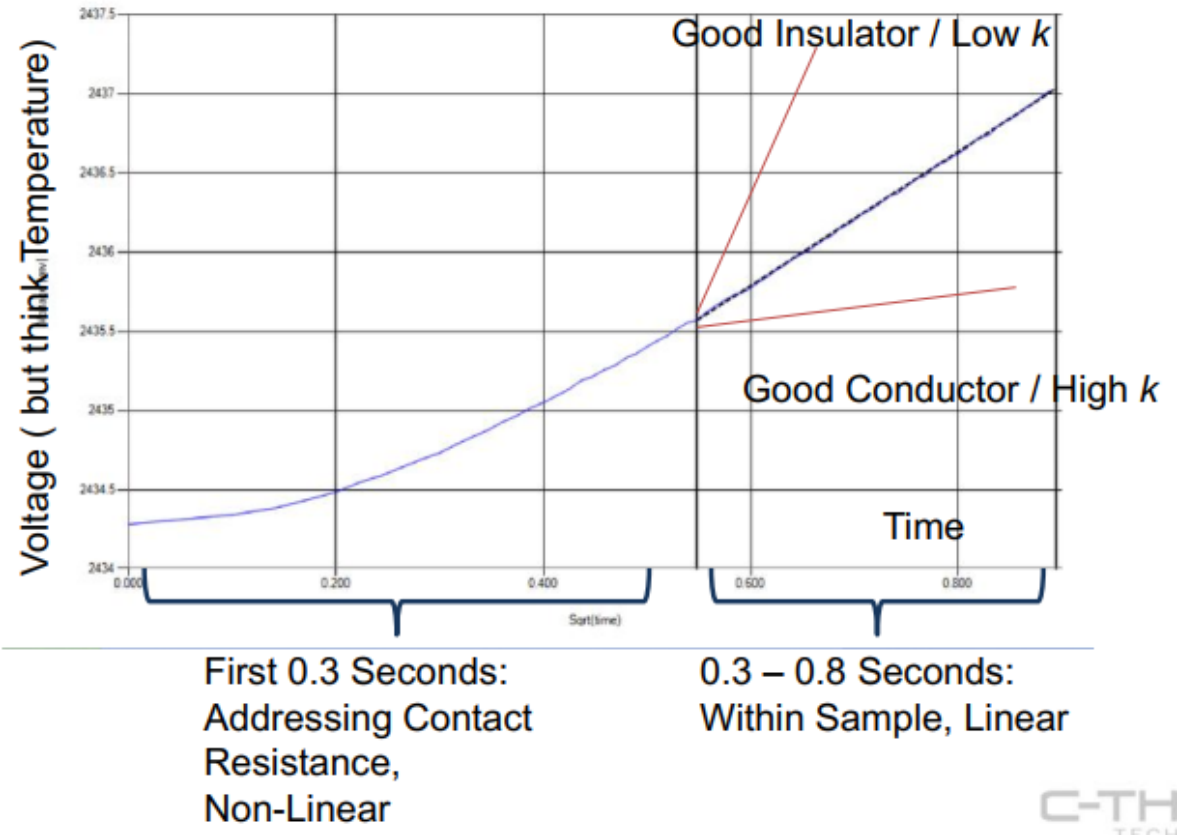

Figure_3.2 Graph of voltage versus time showing how the change in temperature affects the conductivity of the TCi sensor [19]

Laptop with the C-Therm TCi software

A computer system with installed specific C-Therm TCi software interface is also provided. The software package has a relational database with the ability to import and export data and can help in calculating other thermophysical properties such as density, specific heat capacity, diffusivity, depth of penetration, etc. indirectly with some additional inputs of data. The software also acts as a source of communication between the thermal chamber and the TCi thermal controller when experiments are performed at elevated temperature or when the control method is applied.

Tenney thermal chamber

The thermal chamber used is Tenney Jr. thermal chamber with Watlow F4 controller. It is required when the experiment needs to be performed at a temperature other than the room temperature or pressure, also when the automatic control method needs to be applied. The

temperature in the chamber is controlled by the circulation of air which is produced by a propeller type fan driven by an externally mounted motor. To increase the temperature, the chamber air is recirculated through low-mass, open-air nichrome wire heater elements in the conditioning plenum. To prevent direct radiation of heat, the plenum is placed in the ceiling of the chamber and is secluded from the workspace. In the same way, to decrease the temperature, chamber air is recirculated through a refrigerated cooling coil in the conditioning plenum.

Please note that while performing tests in a thermal chamber there is a chance of electrical leakage to pass from thermal chamber floor to the sensor which can impact the results of the test and also can damage the sensor at some point so it is necessary to put a silicon mat between the sensor base plate and the floor of the thermal chamber. Since silicon rubber is electrically insulative material, it will prevent electrical leakage. Also, while applying the control method, keep in mind that the sensor should not be heated or cooled at a rate of more than 5 degrees per minute to prevent the sensor from damaging. Generally to get better results, it is recommended to give 1-hour of ramp time (to increase the temperature to 10 degrees) and then half an hour of soak time. The control method used is shown in the figure below.

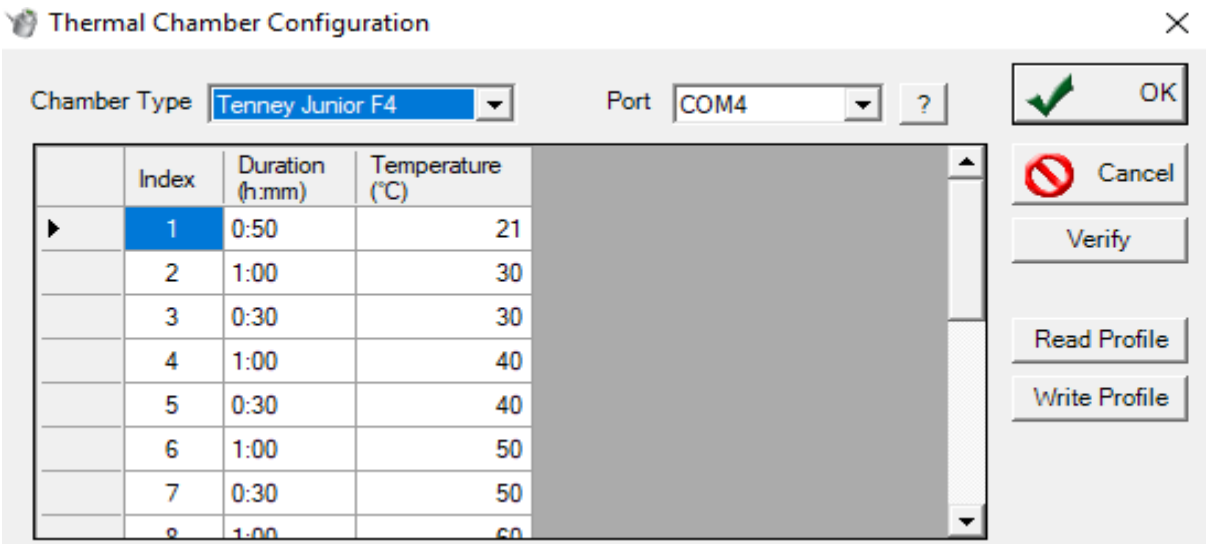

Figure_3.3 Control method

3.1.2 Experimental procedure

In our case, we are going to measure the thermal conductivity of the liquid mixtures and powders. It is recommended to do a reference test with distilled water or any other reference material before beginning the test the desired material.

Testing of powders

To perform the test on the small volume test kit, the following steps are to be followed:

Step 1 Cleaning the sensor

Before starting the experiment, make sure that the sensor surface is clean and dry. If not, then clean the sensor surface with “thermal material remover” and “thermal surface purifier” and then dry it with soft tissue or cloth.

Step 2 Preparing the sample

The next step is taking the sample for measurement. The amount of the sample to be taken is very critical. If the sample amount is more, there will be more compaction when weight is applied as compared to the less amount of sample. So, it is crucial to define a specific amount of sample to be used in all experiments to have consistent results. The following procedure should be followed:

- Fill the 1/8 tsp (0.63 mL) of the powder to be tested scrap off the excess powder with a spatula and transfer it into the weighing dish
- Repeat the above process three times for total volume of specimen
- Carefully pour the sample into the test cell ensuring there are no trapped air bubbles near the surface of the sensor
- Place weight onto the sample so that it seats on the rim of the test cell
- Set the silicone pad and baseplate inside the thermal chamber
- Place the TCi sensor on the base plate as shown in the figure below

Figure_3.4 Small volume test kit with weight on top placed inside the thermal chamber

Step 3 Setting up control

For a test to run automatically at different temperatures, control method needs to be specified. Control method defines the ramp and soak time at certain temperature, and it depends on the type of sample. For good conductors, ramp time should be less as compared to the bad conductors. Also moving from 20 to 30°C requires less ramp and soak time than moving from 70 to 80°C because of thermal stability at lower temperatures.

Step 4 Starting the test

The last step is starting the test. For that first, select a new test button from the toolbar on the computer and then select the project or name the project just to have a proper record of the set of tests performed. After that, we need to define the test method. In the test method, depending upon the project and the sample, we need to choose the calibration method. Calibration methods are usually provided by the manufacturer, and for powders and liquids we have to select “Liquids and Powders HR.” We can also use some other parameters like defining the number of measurements and delay before taking the first measurement etc. If there are no certain requirements, we just go with the default settings. The test method is shown in a figure below:

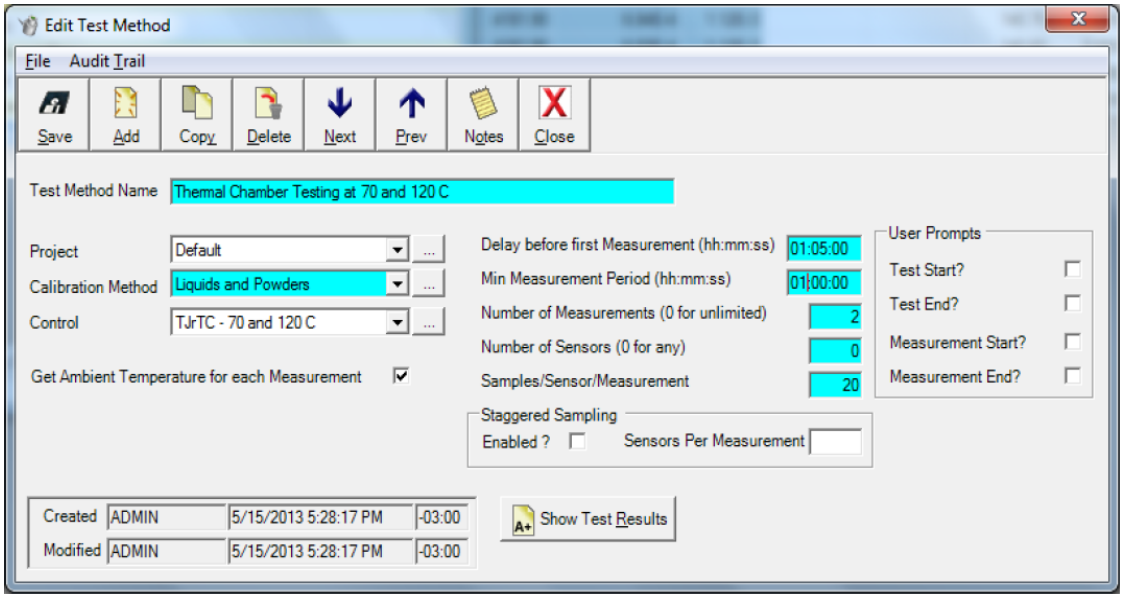

Figure_3.5 Test method

After that, specify the material group and name of the material to be tested and click next. It will take us to the window where we can see the number of the TCi instrument and the name of the sensor to perform the test which is H404. Finally, click the start button to run the test.

Step 5 Data analysis

After the completion of the test, data present on the software can be copied to Excel by copying to the clipboard or exporting to a CSV file that can be then imported to Excel to do analysis. For highly homogeneous powders the relative standard deviation of thermal conductivity measurements of several consecutive specimens of the same material should typically be less than 1 %. The test report can also be generated and is of the following form:

#	Repeat	Sensor ID	Start Time	Effusivity $\frac{W^*\sqrt{(s)}}{(m^2)^*K}$	Conductivity(W/mK)	Ambient T (°C)	DeltaT (°C)	V0 (mV)
1	1	H134	12:55:53	162	0.060	23.21	1.98	3,584.25
2	1	H134	12:57:40	162	0.060	23.26	1.98	3,584.39
3	1	H134	12:59:28	162	0.060	23.27	1.98	3,584.59
4	1	H134	13:01:15	164	0.060	23.26	1.98	3,584.78
5	1	H134	13:03:02	162	0.060	23.28	1.98	3,584.94
6	1	H134	13:04:49	163	0.060	23.29	1.98	3,585.07
7	1	H134	13:06:36	163	0.060	23.29	1.98	3,584.93
8	1	H134	13:08:23	162	0.060	23.30	1.98	3,585.00

Figure_3.6 Test report

Testing of liquids

The testing procedure of liquids is almost the same except the amount of sample. Following steps are to be followed:

Step 1 Cleaning the sensor

Clean the sensor surface with “thermal material remover” and “thermal surface purifier” and dry it.

Step 2 Preparing the sample

- Fill the 1/4 tsp (1.25 mL) of the total liquid volume of specimen
- Transfer this volume directly to the test cell
- Place weight onto the sample so that it seats on the rim of the test cell
- Place the test kit in the thermal chamber to avoid external environmental factors and to equalize the temperature

Step 3 Setting up control

Specify the control method and define the ramp and soak time at certain temperature depending on the type of sample.

Step 4 Starting the test

- Click new test button from the toolbar on the computer
- Select the project or name the project just to have a proper record of the set of tests performed
- Specify the test method and control for the thermal chamber
- Specify the material group and name of the material
- Select the TCi instrument
- Identify the sensor H404
- Click the start button to run the test

Step 5 Data analysis

At the end of the test, copy data to Excel and do analysis. The relative standard deviation of thermal conductivity measurements of several consecutive specimens of the same material should be less than 1 %.

3.2 Specific heat capacity calculation

The specific heat capacity of the mixtures can be calculated indirectly by C-Therm TCi from the measured effusivity and thermal conductivity and input density value. The formula is given below:

$$Specific\ heat\ capacity = \frac{thermal\ effusivity(e)^2}{Thermal\ conductivity(k) * density(\rho)}\ [\frac{J}{kg*K}] \qquad (3.1)$$

The density must be entered to calculate this value, which is measured using the Anton Paar density meter, which employs the oscillating U-tube principle. U-shaped tube is mounted on a counter mass measures the inertial mass of a known volume. The procedure is quite simple. We took the known volume of sample in a syringe and filled the U-tube of the density meter with it from the inlet. The desired temperature is set from the digital screen, and then the test is started. Inside the apparatus, U-tube is excited and starts to oscillate. The characteristic frequency of the U-tube differs depending on the filled in the sample. Density is determined by measuring the change in frequency. The low density is related to high frequency and vice versa. Before taking the next measurement with different sample the cleaning of U-tube should be done by filling in acetone and white spirit and then blowing the air.

CHAPTER 4

EXPERIMENTAL RESULTS AND DISCUSSION

The results of the experiments to measure thermophysical properties of the water-based mud and oil-based mud and their components are discussed in this chapter. The temperature dependency of these properties is vital for heat transfer calculations. Experiment on each component is performed thrice, and the average values of the test results are being presented here.

4.1 Base components and mixtures

Thermal conductivity tests are performed separately on some of the base components and their solutions with water. Base components are in the powder form, and it is seen that because of the presence of interstitial air in powders the thermal conductivity is reduced to a greater extent as compared to the solid form of the same material. Following are the components being tested:

Distilled water

Distilled water is the reference material, and the following table shows the thermal conductivity value of distilled water from 20 to 80°C.

Table_4.1

Temperature T (°C)	Thermal Conductivity k, (W/mK)
20	0.608
30	0.620
40	0.630
50	0.634
60	0.638
70	0.642
80	0.647

The plot in figure 4.1 shows that the thermal conductivity of distilled water increases with temperature increase. The forecast is also shown in the plot, and the following equation can be used to calculate the thermal conductivity of distilled water.

$$k = 0.0272 \ln(T) + 0.5274 \quad [W/mK] \tag{4.1}$$

The variation in the value of thermal conductivity can be calculated as:

$$Thermal\ conductivity\ variation(\%) = \frac{k_{max} - k_{min}}{k_{min}} * (100) \tag{4.2}$$

where,

k_{max} = maximum thermal conductivity of the sample in the given data

k_{min} = minimum thermal conductivity of the sample in the given data

For distilled water it is calculated as: $(\frac{0.647-0.608}{0.608})(100)$ = 6.4 %.

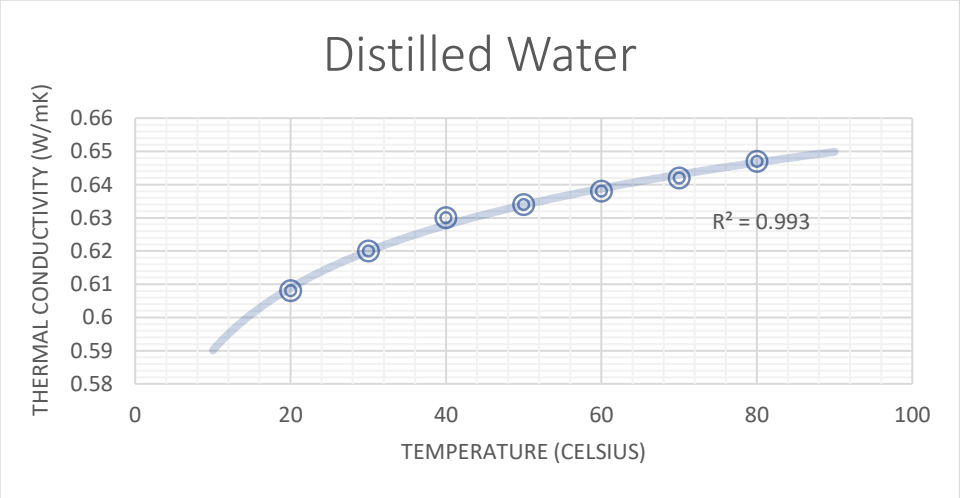

Figure_4.1 Measured thermal conductivity of distilled water

Potassium chloride

It is one of the base components used in the water-based mud. Thermal conductivity values of potassium chloride are showed in the table below.

Table_4.2

Temperature T (°C)	Thermal Conductivity k, (W/mK)
20	0.126

30	0.125
40	0.123
50	0.120
60	0.119
70	0.117
80	0.115

Thermal conductivity of potassium chloride decreases with the increase in temperature, and the following linear equation can be used to describe the relation. Variation in thermal conductivity is 9.56 percent.

$$k = -0.0002(\mathrm{T}) + 0.1302 \quad [W/mK] \tag{4.3}$$

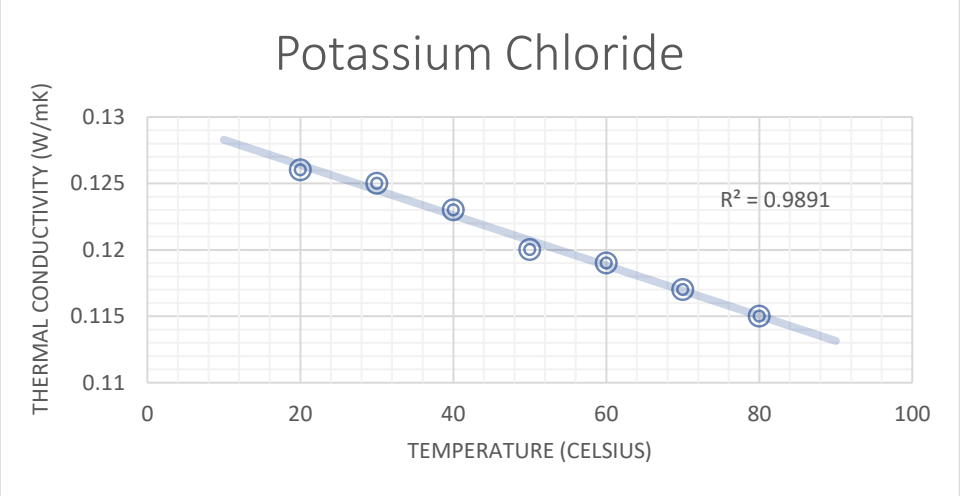

Figure_4.2 Measured thermal conductivity of potassium chloride

Calcium chloride

The important base component used in the oil-based mud is calcium chloride. Its value increases a bit until 40°C after which it changes its phase and turns to solid form, which results in a dramatic increase of its thermal conductivity to 0.431 as shown in the table below.

Table_4.3

Temperature T (°C)	**Thermal Conductivity k, (W/mK)**

25	0.107
30	0.106
40	0.112
50	0.431
60	0.444
70	0.448
80	0.453

The plot in figure 4.3 shows the strange trend of thermal conductivity of calcium chloride with temperature increase. Following equations are used to determine the thermal conductivity of calcium chloride:

$$k = \begin{matrix} 0.0004(T) + 0.0966 & T \leq 40 \\ 0.0007(T) + 0.3985 & T \geq 43 \end{matrix} \quad (4.4)$$

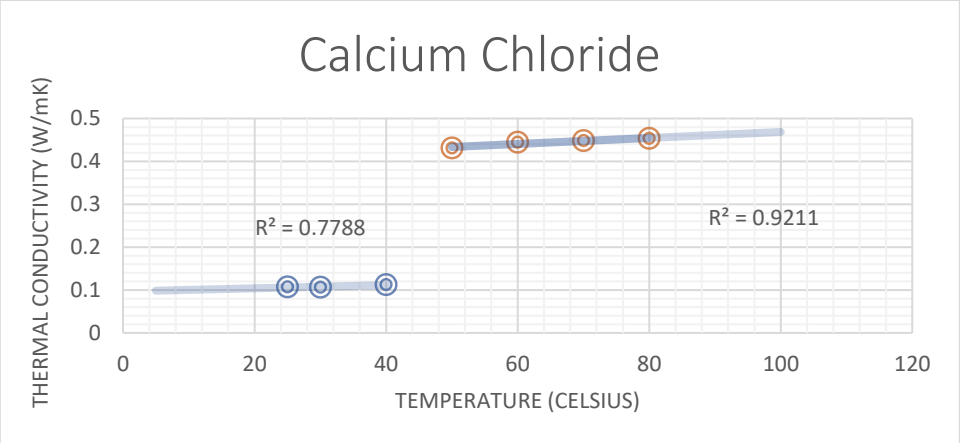

Figure_4.3 Measured thermal conductivity of calcium chloride

Barite

Barite is the weighing material used in both oil-based mud and water-based mud to increases the hydrostatic pressure of the drilling mud, allowing it to compensate for high-pressure zones experienced during drilling. It also acts as a lubricant because of its softness. It's thermal conductivity values at different temperatures are shown in a table below.

Table_4.4

Temperature T (°C)	Thermal Conductivity k, (W/mK)
25	0.0949
30	0.0948
40	0.0939
50	0.0929
60	0.0920
70	0.0908
80	0.0901

The figure below shows the decreasing trend of thermal conductivity of barite with temperature increase. A linear equation is used to determine the relation which is given below in equation 4.5. The variation in the thermal conductivity of barite is 5.32 percent.

$$k = -9E - 05(T) + 0.0974 \quad [W/mK] \tag{4.5}$$

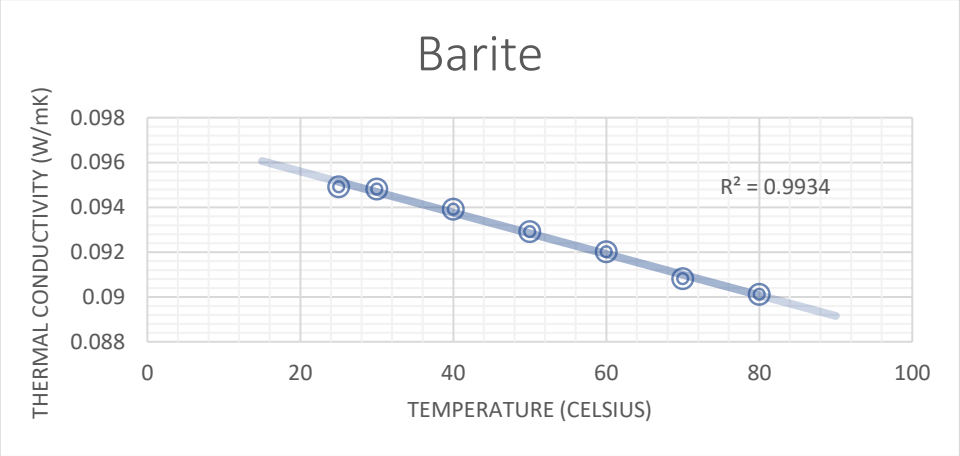

Figure_4.4 Measured thermal conductivity of barite

Bentone 128

Bentone 128 is added in oil-based mud to enhance stability and dispersibility. It is a fast yielding viscosifier which yields effectively at reduced shear. Thermal conductivity values of Bentone 128 are given in Table 4.5.

Table_4.5

Temperature T (°C)	Thermal Conductivity k, (W/mK)
20	0.0782
30	0.0788
40	0.0919
50	0.1038
60	0.1042

Thermal conductivity of Bentone 128 increases slightly with the increase in temperature, and the following equation can be used to calculate the thermal conductivity of Bentone 128. The variation in the value of thermal conductivity of Bentone 128 is 33.24%.

$$k = -0.0002(\mathrm{T}) + 0.1302 \quad [W/mK] \tag{4.6}$$

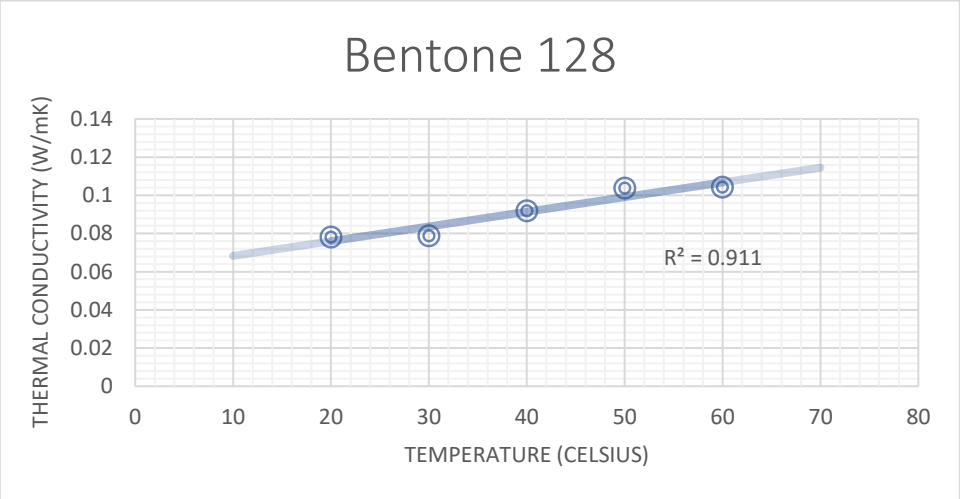

Figure_4.5 Measured thermal conductivity of Bentone 128

Base Oil

It is an important component of oil-based mud, and its thermal conductivity values from room temperature to 80°C are given in the table below.

Table_4.6

Temperature T (°C)	Thermal Conductivity k, (W/mK)
22	0.1321
30	0.1309
40	0.1294
50	0.1278
60	0.1262
70	0.1244
80	0.1225

The figure below shows the decreasing trend of thermal conductivity of base oil with temperature increase. A linear equation is used to determine the thermal conductivity of base oil, which is given below. Standard deviation is 7.83 percent.

$$k = -0.0002(T) + 0.1359 \quad [W/mK] \tag{4.7}$$

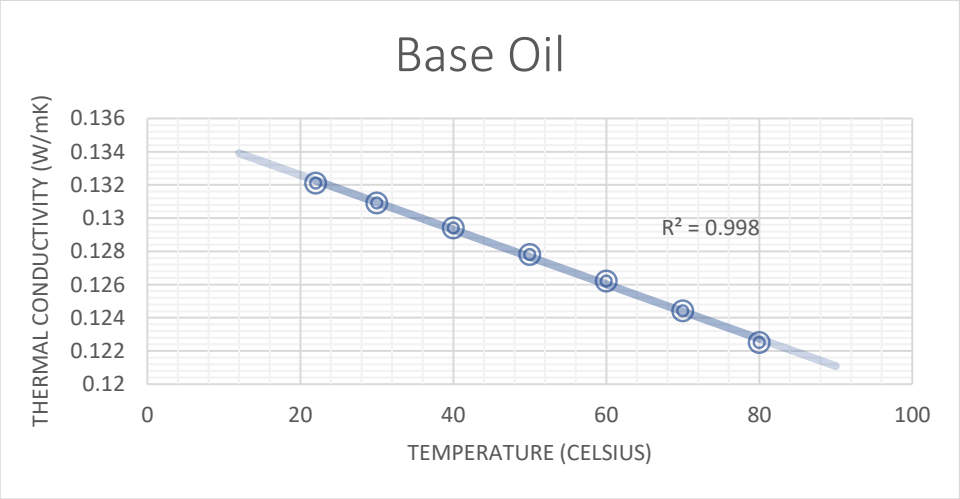

Figure_4.6 Measured thermal conductivity of base oil

Sand

Sand from the cuttings generated during drilling mixed in the drilling mud and it impacts the thermophysical properties of the drilling fluid. An experiment is performed on the sand of

particle size less than 45 micrometers. Thermal conductivity of sand at different temperatures is shown in the table below.

Table_4.7

Temperature T (°C)	**Thermal Conductivity k, (W/mK)**
21	0.1098
30	0.1095
40	0.1092
50	0.1090
60	0.1088
70	0.1086
80	0.1084

The figure below shows the decreasing trend of thermal conductivity of sand with temperature increase. The linear equation used to describe this relationship is given below. The variation in the thermal conductivity values for sand is only 1.01 percent.

$$k = -2E-05(T) + 0.1102 \quad [W/mK] \tag{4.8}$$

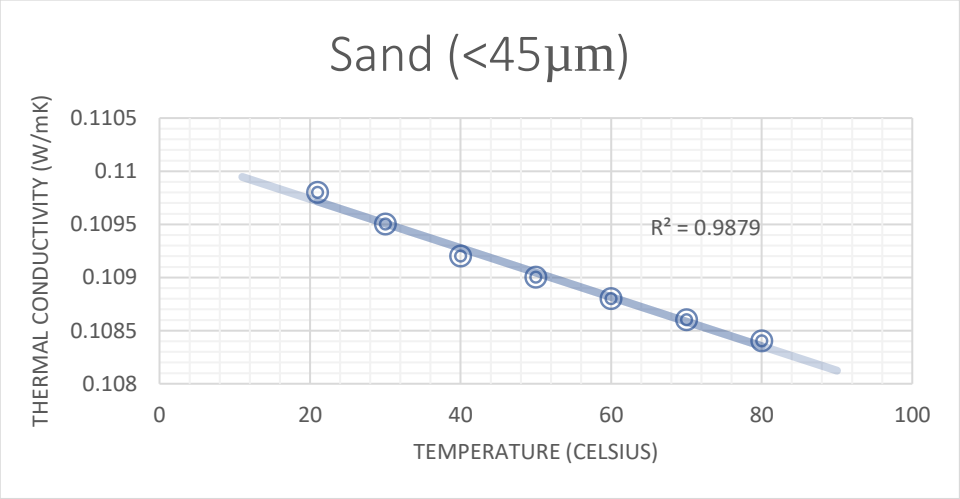

Figure_4.7 Measured thermal conductivity of sand

Calcium chloride and water mixture

The test is performed to measure the thermal conductivity of the mixture of calcium chloride with water. The mixture contains 22 percent calcium chloride and 78 percent water. The values are given in the table below.

Table_4.8

Temperature T (°C)	Thermal Conductivity k, (W/mK)
23	0.4611
30	0.4529
40	0.4132
50	0.3942
60	0.3765
70	0.4037
80	0.2922

Figure 4.8 shows the trend lines of thermal conductivity of calcium chloride and water mixture with the increase in temperature. A mixture of calcium chloride and water also has less value of thermal conductivity than that of water. The variation of the thermal conductivity values for calcium chloride and water solution is 57.80 %. The forecast is also shown in the plot, and the equation to describe this trend is given below:

$$k = -0.0024(T) + 0.5186 \quad [W/mK] \tag{4.9}$$

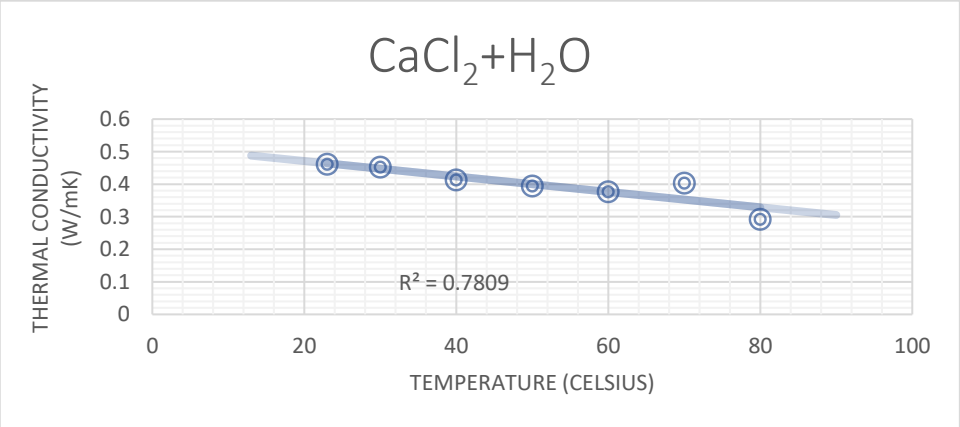

Figure_4.8 Measured thermal conductivity of calcium chloride and water solution

Potassium chloride and water mixture

A mixture of potassium chloride and water gives less value of thermal conductivity than that of water when the test is performed. The mixture contains 14 percent potassium chloride and 86 percent distilled water. The mixture is highly unstable, and it is difficult to judge its thermal conductivity value at a higher temperature. Following table shows the value of thermal conductivity from room temperature to 40°C.

Table_4.9

Temperature T (°C)	**Thermal Conductivity k, (W/mK)**
22	0.5221
25	0.5269
30	0.5279
35	0.5292
40	0.5373

The trend line along with forecast of experimental values of thermal conductivity of potassium chloride and water mixture with the increase in temperature is given in figure 4.9. Variation in thermal conductivity values is 2.9 percent. The equation to describe our experimental trend is linear and is given as:

$$k = 0.0007(T) + 0.5072 \quad [W/mK] \tag{4.10}$$

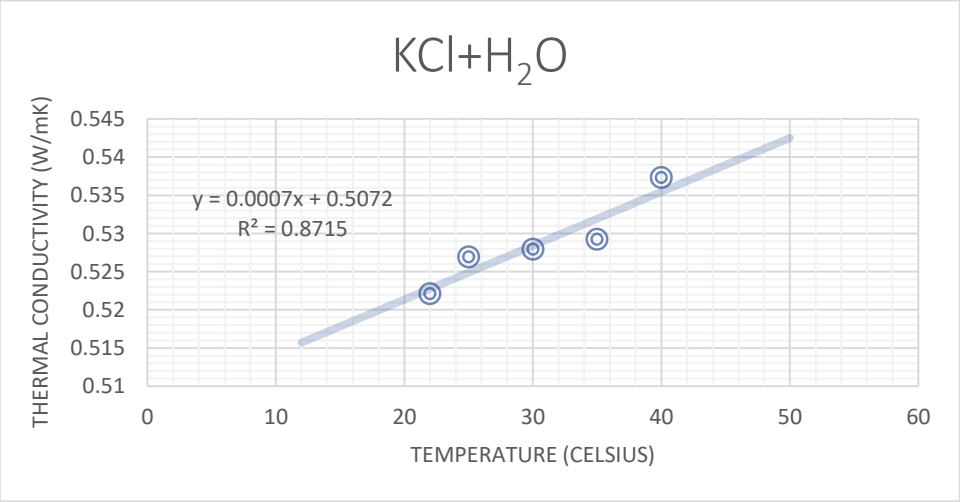

Figure_4.9 Measured thermal conductivity of potassium chloride and water solution

Table below shows the sensitivity of thermal conductivity value of each material described above with the temperature change. We can see that values of thermal conductivity for calcium chloride solution with water and Bentone 128 is the most sensitive to temperature and sand is the least sensitive. This means with the increase in temperature the value of thermal conductivity of Bentone 128 increases a lot that is from 0.0782 to 0.1042 and for sand the change in value is least that is from 0.1098 to 0.1084.

Table_4.10

Material	**Variation in Thermal Conductivity (%)**
Distilled Water	6.4
KCL + H_2O	2.9
$CaCL_2$ + H_2O	57.80
Barite	5.32
Bentone 128	33.24
EDC 99	7.83
Sand	1.01
KCL	9.56

From the table above it can be seen that variation in thermal conductivity for KCL is 9.56 percent and of distilled water is 6.4 percent but if you look at the variation of thermal conductivity for potassium chloride and water solution, it is only 2.9 percent. This means that trend of thermal conductivity changes when different components are mixed together and you can not just estimate the values using general models like Tsederberg method. Our model which is based on experimental values at different temperatures consider the reaction kinetics and gives the accurate thermal conductivity value of the solution.

4.2 Unweighted Water-based Mud

Water-based mud of density 1085 $^{kg}/_{m^3}$ is prepared with the following components:

Table_4.11

Fresh Water	420.95 grams
KCL	60 grams
Soda Ash	0.5 grams
Duo Tec NS	2 grams
Troll FL	5 grams
Glydril MC	15 grams

Specific heat capacity test is performed on unweighted water-based mud, and we can have the following values:

Table_4.12

Temperature T (°C)	**Specific heat capacity c, (J/kg*K)**
20	3453.61
30	3563.88
40	3628.38
50	3713.41
60	3757.11

The following figure shows the trend of specific heat capacity of unweighted water-based mud with the forecast. Variation in specific heat capacity is calculated as 8.78 percent, and the resulting linear equation is used to describe this experimental trend:

$$C_p = 7.56534(T) + 3320.7 \quad [{}^{J}/_{kg*K}] \tag{4.10}$$

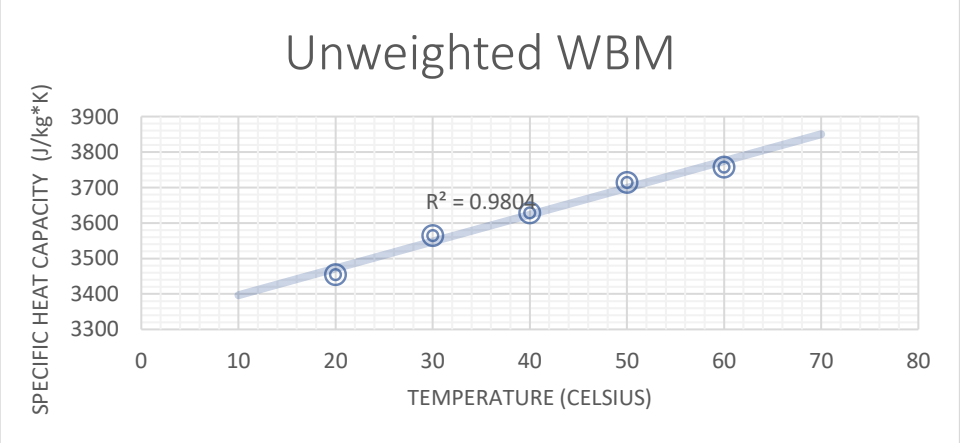

Figure_4.10 Measured specific heat capacity of unweighted water based mud

Thermal conductivity data of the unweighted water-based mud is given in the table below

Table_4.13

Temperature T (°C)	Thermal Conductivity k, (W/mK)
20	0.4650
30	0.4955
40	0.5120
50	0.5349
60	0.5594

Thermal conductivity of the unweighted water-based mud increases with the increase in temperature, as shown in the figure below with the forecast. Variation in the values of thermal conductivity of water-based mud is 20.3 percent and the following linear equation used to describe this trend is given as:

$$k = 0.0023(T) + 0.4221 \quad [W/mK] \tag{4.11}$$

The model is developed based on the experimental values of thermal conductivity within the temperature range 10°C to 60°C due to the sensor design limit therefore the model is valid only in that temperature range. Out of such range, the extrapolation might lead to big errors on specific heat and thermal conductivity.

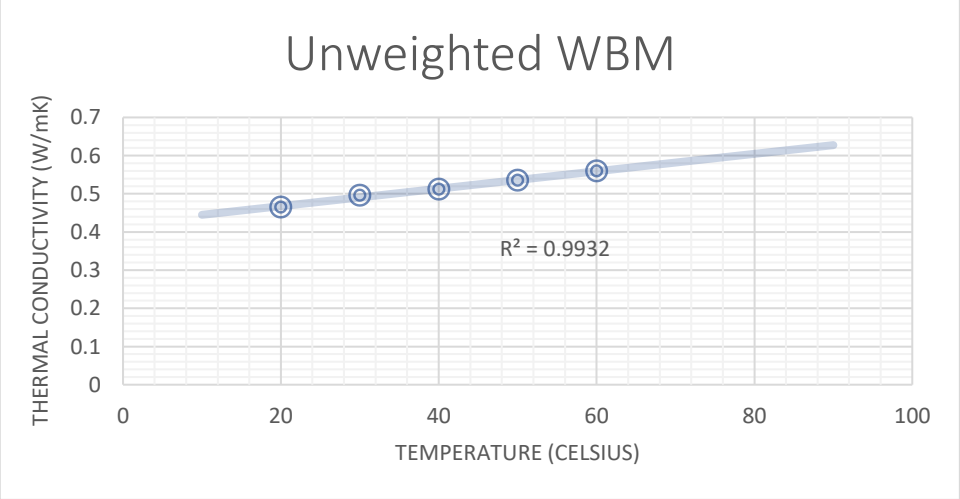

Figure_4.11 Measured thermal conductivity of unweighted water based mud

Now we will compare our experimental result with Tsederberg method and Churchill method. The values of thermal conductivity calculated by these three methods are shown in a table below:

Table_4.14

Temperature T (°C)	**Experimental Equation (4.11)**	**Tsederberg Method Equation (2.5)**	**Churchill Method Equation (2.9)**
20	0.4681	0.5482	0.4590
30	0.4911	0.5586	0.4667
40	0.5141	0.5671	0.4727
50	0.5371	0.5702	0.4742
60	0.5601	0.5736	0.4765

Following graph shows the trend of thermal conductivity of unweighted water-based mud along with a forecast from three different models. If we look at the individual components of the water-based mud the major ones are fresh water and potassium chloride. As seen in the figure 4.1 fresh water has inreasing trend of thermal conductivity of thermal conductivity with rise in temperature and potassium chloride has the opposite trend as per figure 4.2. Tsederberg and Churchill model has almost the straight line for unweighted water-based mud as shown in figure 4.12 however our experimental model has higher slope and is more sensitive to the temperature and gives accurate values.

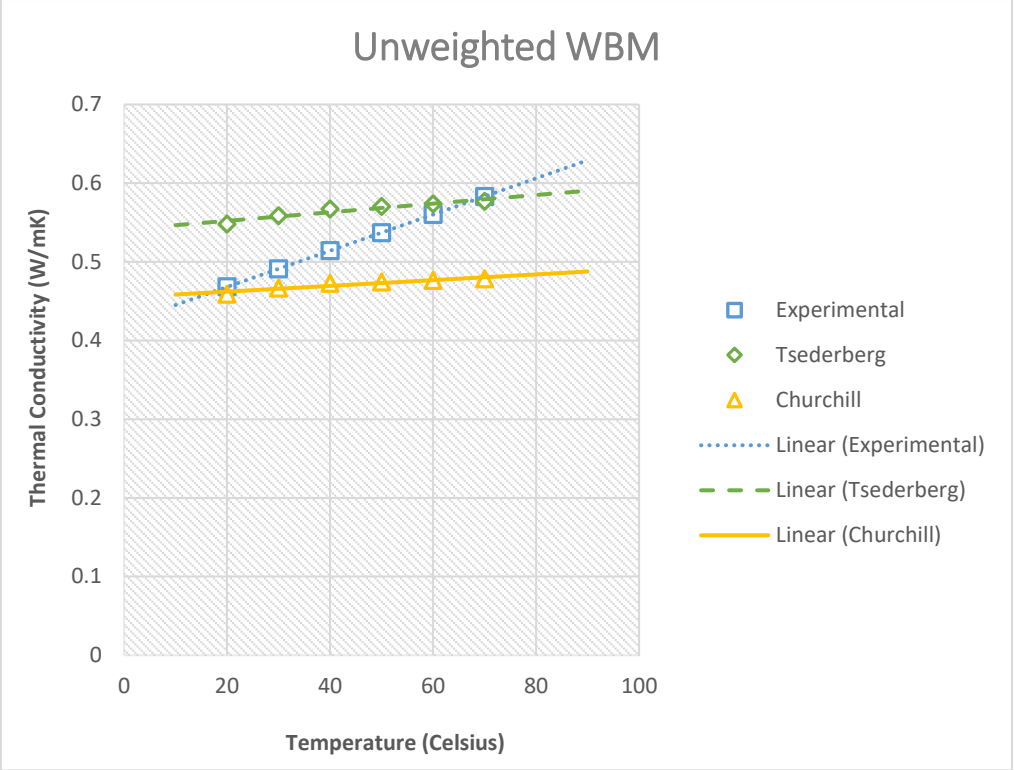

Figure_4.12 Thermal conductivity comparison of Churchill, Tesederberg and experimental model for water based mud

4.3 Unweighted Oil-based Mud

Oil-based mud of density 935 $^{kg}/_{m^3}$ has the following composition:

Table_4.15

Fresh Water	103.6 grams
EDC 99	254.4 grams
Lime	10 grams
OneMul NS	10 grams
Bentone 128	7.5 grams
VersaTrol M	3.5 grams
CaCl2	29.85 grams

Oil-based unweighted mud is more stable than the unweighted water-based mud. The specific heat capacity values of unweighted oil-based mud are given in the table below.

Table_4.16

Temperature T (°C)	**Specific heat capacity c, (J/kg*K)**

23	2135.61
30	2154.88
40	2172.38
50	2179.10
60	2171.73
70	2165.41
80	2150.11

The specific heat capacity values of unweighted oil-based mud increase with the increase in temperature until 60°C after that it will start decreasing with the increase in temperature as shown in the figure below. Following polynomial equation is used to describe this trend.

$$C_p = -0.0426(T^2) + 4.5735(T) + 2055 \quad [{}^{J}/_{kg * K}] \tag{4.12}$$

It is noted that the specific heat capacity of oil-based mud is less than that of water-based mud.

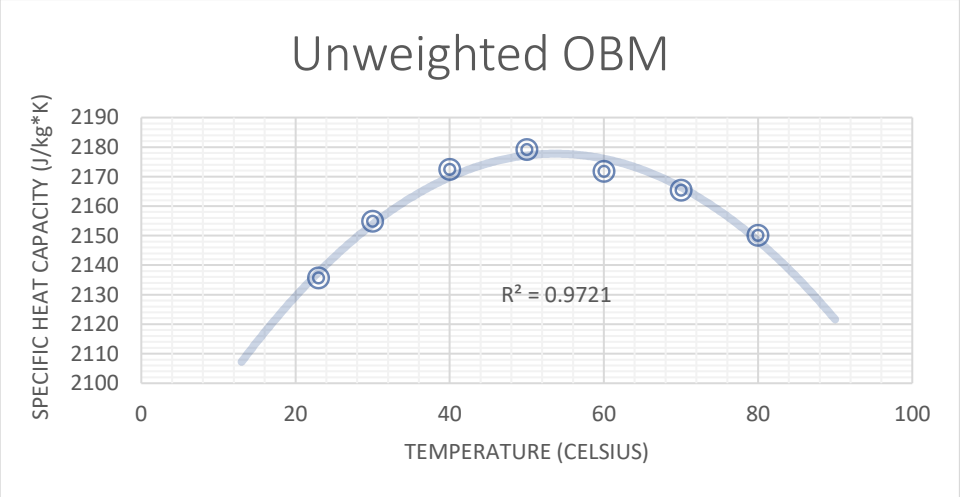

Figure_4.13 Measured specific heat capacity of oil based mud

Thermal conductivity of the unweighted oil-based mud decreases slightly with the increase in temperature. This verifies our model result as thermal conductivity trend of base oil (figure 4.6) and of calcium chloride and water solution (figure 4.8) which are the main component in oil-based mud are also decreasing with the increase in temperature. The experimental values of thermal conductivity of oil-based mud are given in the table below.

Table_4.17

Temperature T (°C)	Thermal Conductivity k, (W/mK)
20	0.1911
30	0.1908
40	0.1907
50	0.1902
60	0.1895
70	0.1891
80	0.1883

Figure 4.13 shows the trend of thermal conductivity of the unweighted oil-based with the increase in temperature. Variation in the thermal conductivity values with the increase in temperature is only 1.3 percent. A polynomial equation is used to describe this trend, which is given as:

$$k = -6E-07(T^2) + 2E-05(T) + 0.1908 \quad [W/mK] \tag{4.13}$$

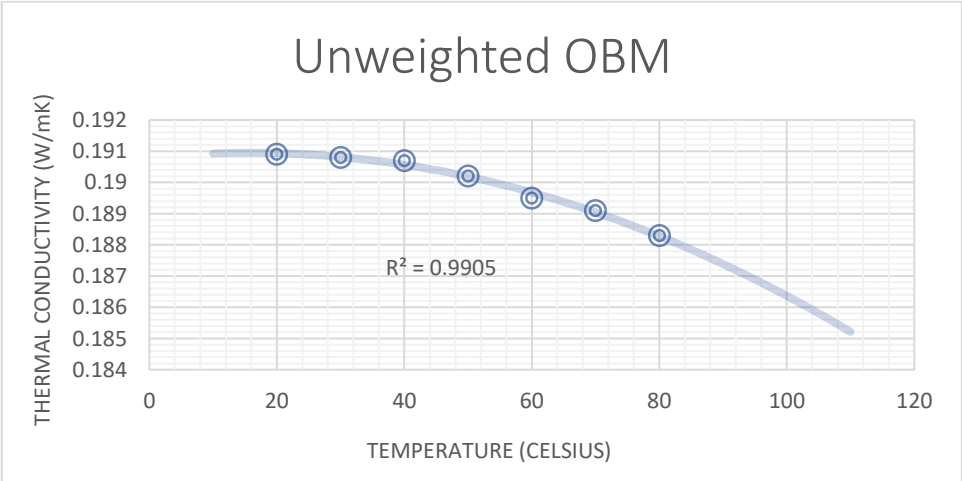

Figure_4.14 Measured thermal conductivity of oil based mud

Now our experimental results are compared with Tsederberg method and Churchill method. The values of thermal conductivity calculated by these three methods are shown in a table below:

Table_4.18

Temperature T (°C)	Experimental Equation (4.13)	Tsederberg Method Equation (2.5)	Churchill Method Equation (2.9)
20	0.1909	0.2563	0.2367
30	0.1908	0.2594	0.2390
40	0.1906	0.2614	0.2419
50	0.1903	0.2860	0.2963
60	0.1898	0.2870	0.2979
70	0.1892	0.2872	0.2982
80	0.1885	0.2877	0.2989

Figure 4.15 shows the trend of thermal conductivity of unweighted oil-based mud along with a forecast from three different models. According to our experimental model, thermal conductivity is decreasing slightly with the increase in temperature as explained before, however if you see the lines of Tsederberg and Churchill model both show an irregular behavior and increasing trend of thermal conductivity values with the increasing temperature because of the presence of Calcium chloride in the mud. As calcium chloride shows irregular behaviour of thermal conductivity with the increase in temperature (figure 4.3). This means that both of these models only consider the individual components and do the estimation of the thermal conductivity value of final mixture. Since such models do not consider the reaction kinetics of the solution thus they are not reliable especially at a higher temperature where the value changes abruptly at around 40 °C as seen from the graph. On the contrary, our model which is developed from the experimental results shows consistent value taking into account the chemistry of solution.

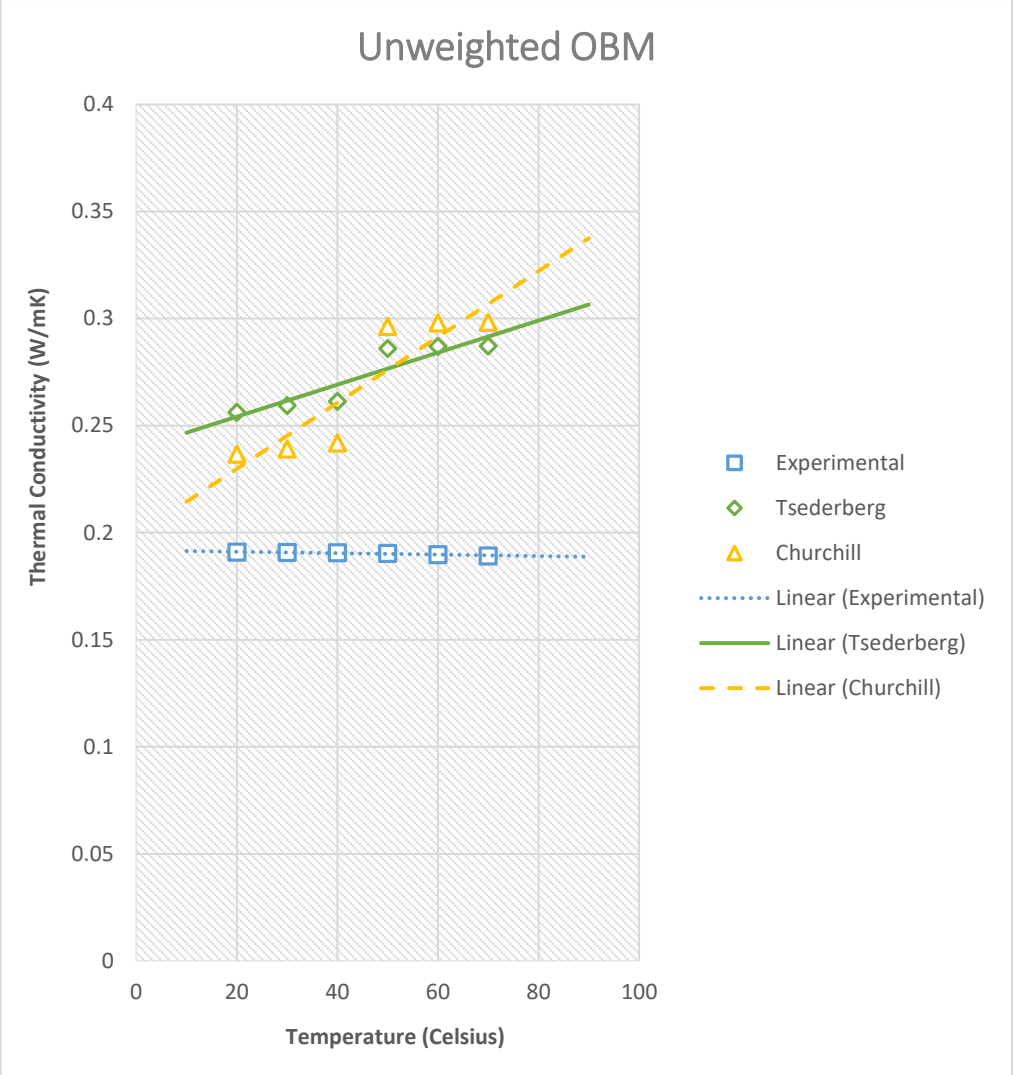

Figure_4.15 Thermal conductivity comparison of Churchill, Tesederberg and experimental model for oil-based mud

CHAPTER 5

CASE STUDY

Case studies on two wells are presented in this chapter. Simulations were performed in the drilling calculator, and the trend of bottom hole temperature was observed. Churchill model was used in drilling calculator for the calculation of thermal conductivity value [9]. Comparison of the results was made between Churchill model and new models developed for calculation of thermal conductivity and specific heat capacity of the oil-based mud and water based mud.

5.1 Drilling calculator

It is a drilling simulator which is based on different wellbore models that are used to give an overview of the current properties of the wellbore and to predict future changes. Simulator gets data from the drilling operation and must contain accurate wellbore models. Drilling calculator consists of the following set of numerical models [14]:

Hydraulic model

A transient hydraulic model determines the pressure distribution inside the wellbore by solving mass and momentum balance. Dynamic effects like pump accelerations, surge, swab, and the presence of various drilling or formation fluids in the well are accounted for by the model [14].

Cuttings transport model

A transient cuttings transport model determines the distribution of the cuttings inside the annulus. It also predicts whether the drilled solids are suspended in the drilling fluid or they are settling down as a cuttings bed. Simulation of the transport of cuttings by bed erosion is also performed [14].

Torque and drag model

A soft torque and drag model is used to calculate the tension and torque distribution along the drill string [14].

Heat transfer model

This is a concerned model which takes thermal conductivity and specific heat capacity as an input value and computes the temperature evolution inside the wellbore and in the near formation. Conductive and convective heat transfer are also accounted for by the simulations.

All the models mentioned above are integrated. The hydraulic model uses the temperature profile, which is generated by the heat transfer to estimate pressures, densities and velocities. Resultant values are then used by the torque and drag model for buoyancy considerations and by the cuttings transport model for estimation of the transport capabilities [14].

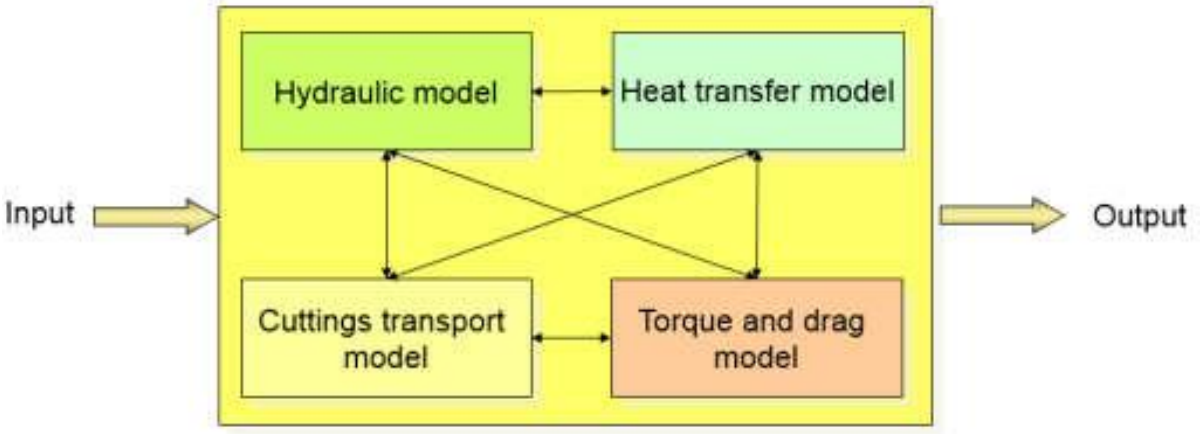

Figure_5.1 Simulator modules and their interaction [14]

5.2 Simulation of horizontal well

The well under consideration is a shallow horizontal well with the geothermal gradient of 12 degrees per 100 meter. Oil-based mud of density 1.15 sg is being used for drilling purpose. Currently well is static and bit depth is 2286 meters while the bottom hole is at 2296 meters measured depth. Well is cased up to 845 meters measured depth with a 9 5/8- inches casing and further drilled up with 8 ½- inches bit.

5.2.1 *Scenario 1*

Three models were used for flow rate analysis. These were the models; Churchilll model, oil-based mud and water-based mud model. Well was circulated at flow rate of 1500 liters per minute until the temperature stabilized. The summary of simulations performed is given in the table below.

Table_5.1

Simulation	Changing Parameter	Value of Changed Parameter
1	Model	Churchill Model
2	Model	OBM Model
3	Model	WBM Model

Annulus temperature profiles for all the three models from casing shoe to the bottom hole are given in figure 5.2. Temperature is plotted against the measured depth at different times. Dotted line indicates the time t1 which represents the beginning of circulation, dash-dot line indicates the time t3 which represents the time at the end of circulation process and dashed line which indicates t2 is the time in the middle of circulation process.

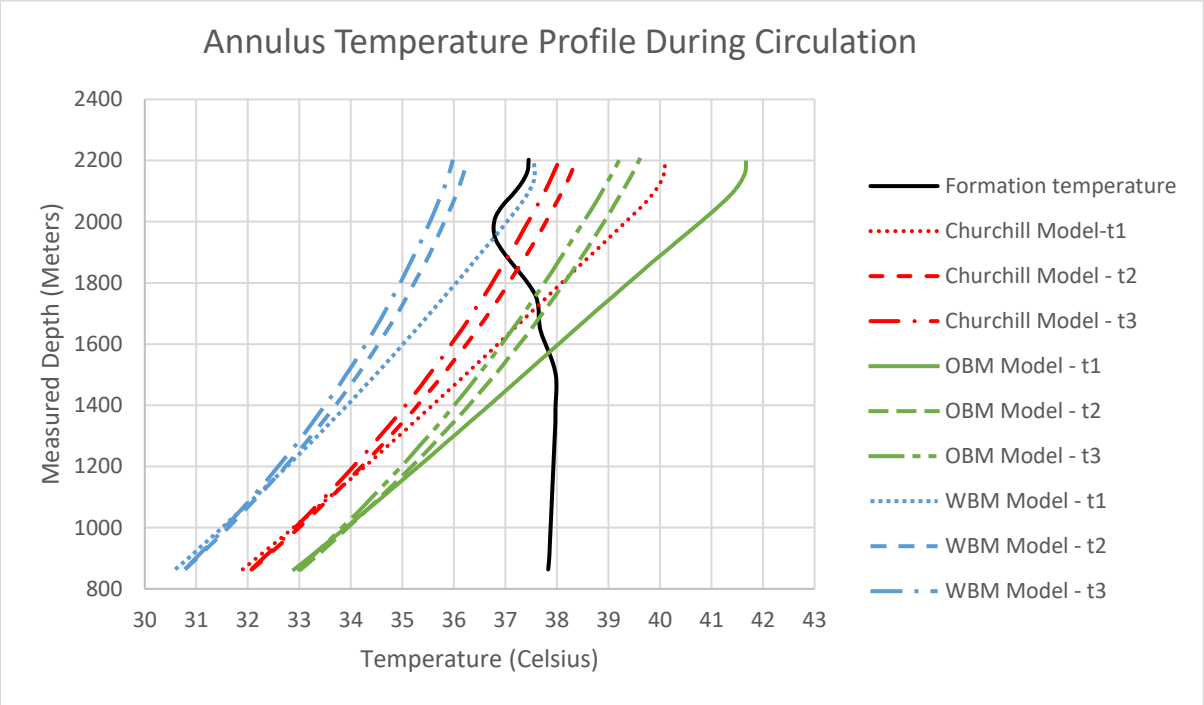

Figure_5.2 Annulus temperature profile during circulation

It can be observed from the figure that all the models follow almost the same trend of temperature variation. At t1 the temperature of annulus is higher and for all the three models it is even higher than the formation temperature. However, due to circulation it starts decreasing. It can be seen that annulus temperature is maximum for the oil-based mud model and minimum for the water-based mud model and for Churchill model it is somewhere in

between. The value of thermal conductivity and specific heat capacity is least for the OBM model and maximum for WBM model. Bottom hole temperature for OBM model at the beginning of circulation is 41.67°C and at the end of circulation it decreases 2.46°C. For Churchill model it is 40.09 at the beginning of circulation and at the end of circulation it decreases to 38.05°C. For WBM model the temperature decrease is from 37.54°C to 35.94°C.

5.2.2 *Scenario 2*

In the second scenario we will do the analysis of different flow rates for the oil based mud model. Well is circulated for more than 1 hour. The summary of simulations performed is given in the table below.

Table_5.2

Simulation	Changing Parameter	Value of Changed Parameter
1	Flow rate	200 lpm
2	Flow rate	1500 lpm
3	Flow rate	2000 lpm

Bottom hole temperature profiles for all the three flowrates are given in figure 5.3. Temperature is plotted against the simulation time.

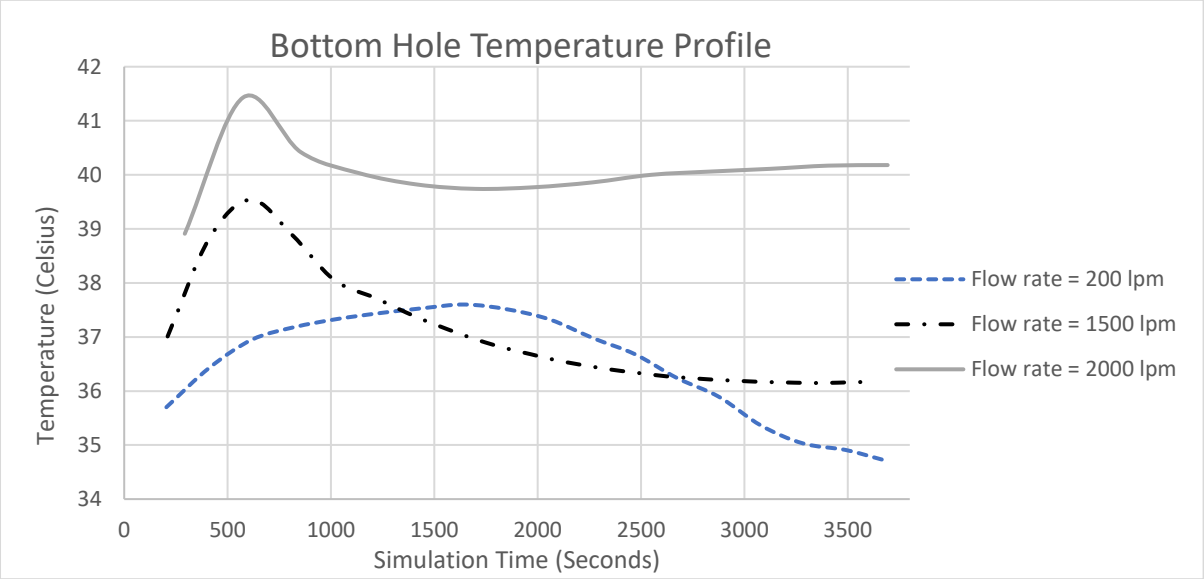

Figure_5.3 Bottom hole temperature profile during circulation at different flow rates

It can be observed from the figure that bottom hole temperature is maximum for the highest flow rate and minimum for the lowest flow rate. At 2000 liter per minute, the bottom hole temperature first increase quickly from 38.91°C to 41.43°C and then it starts to decrease and becomes stable after some time at 40.18°C. Almost similar trend is being seen for the flow rate of 1500 liters per minute where bottom hole temperature increases quickly from 37.01°C to 39.54°C and then starts to decrease and become stable at 36.17°C. For 200 liters per minute, bottom hole temperature increases gradually from 35.69°C to 37.6°C and then decreases slowly to 34.73°C by the end of simulation. Thus we can say that flow rate is important factor for cslculation of the bottom hole temperature.

5.2.3 *Scenario 3*

For the third scenario we will do the analysis of flow rate by varying the inlet temperature for the oil-based mud model. Well is circulated at the rate of 2000 liter per minute for more than one hour. The summary of simulations performed is given in the table below.

Table_5.3

Simulation	Changing Parameter	Value of Changed Parameter
1	Inlet temperature	20 °C
2	Inlet temperature	40 °C

Bottom hole temperature profiles for different inlet temperature is given in figure 5.4. Temperature is plotted against the simulation time. When the inlet temperature is high that is 40°C the bottom hole temperatutre starts to increase suddenly with the circulation however for lower inlet temperature it can be observed from the figure that there is very slight increase in the bottom hole temperature that is from 38.91°C to 40.18°C. However, for inlet temperature 40°C after the circulation bottom hole temperature takes more time to stablise and increases from 39.01°C to 44.73°C. Thus, inlet temperature is also a crucial factor for determining the bottom hole temperature profile.

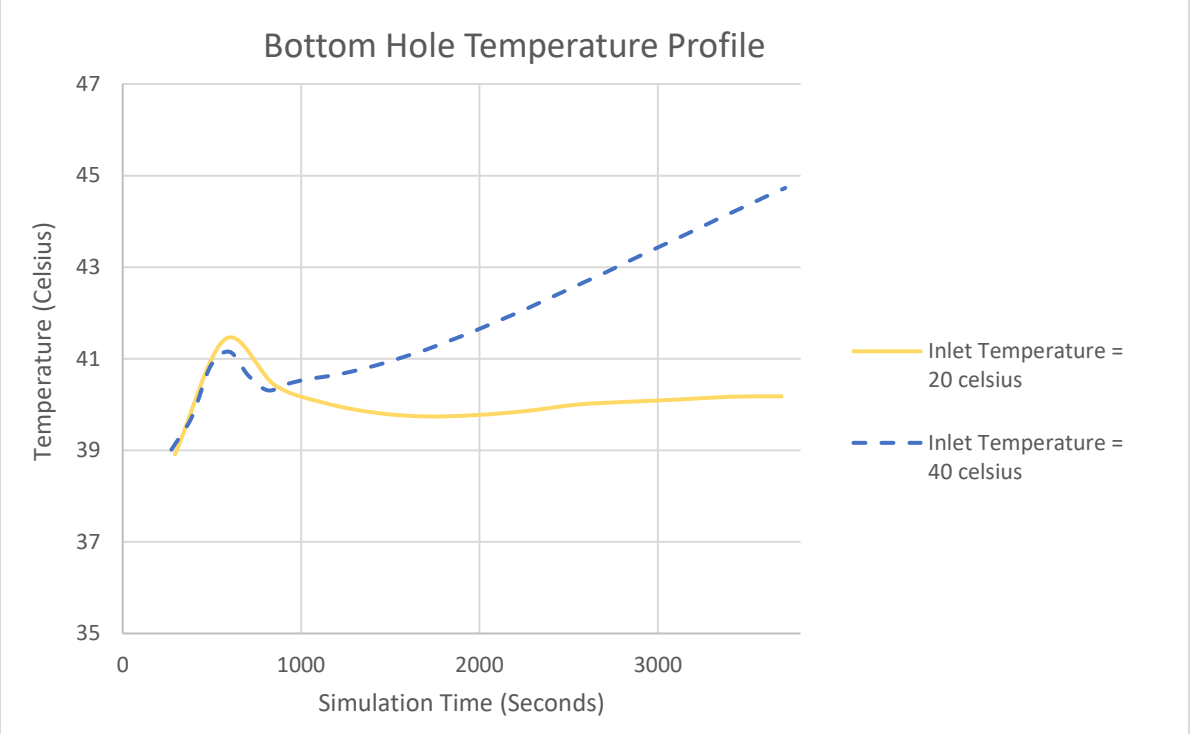

Figure_5.4 Bottom hole temperature profile during circulation at different inlet temperatures

5.2.4 *Scenario 4*

Lastly, we will do the analysis for different rate of penetration for all the three models. For the simulation purpose, well is drilled for 20 meters. The summary of simulations performed is given in the table below.

Table_5.4

Simulation	Changing Parameter	Value of Changed Parameter
1	Rate of Penetration	43.2 meters per hour
2	Rate of Penetration	21.6 meters per hour
3	Rate of Penetration	7.2 meters per hour
4	Model	OBM model
5	Model	WBM model

Annulus temperature profile at the casing shoe and at bottom hole are given in figure 5.5. It can be observed from the figure that all the models follow a similar trend of temperature variation with different rate of penetrations at different depths.

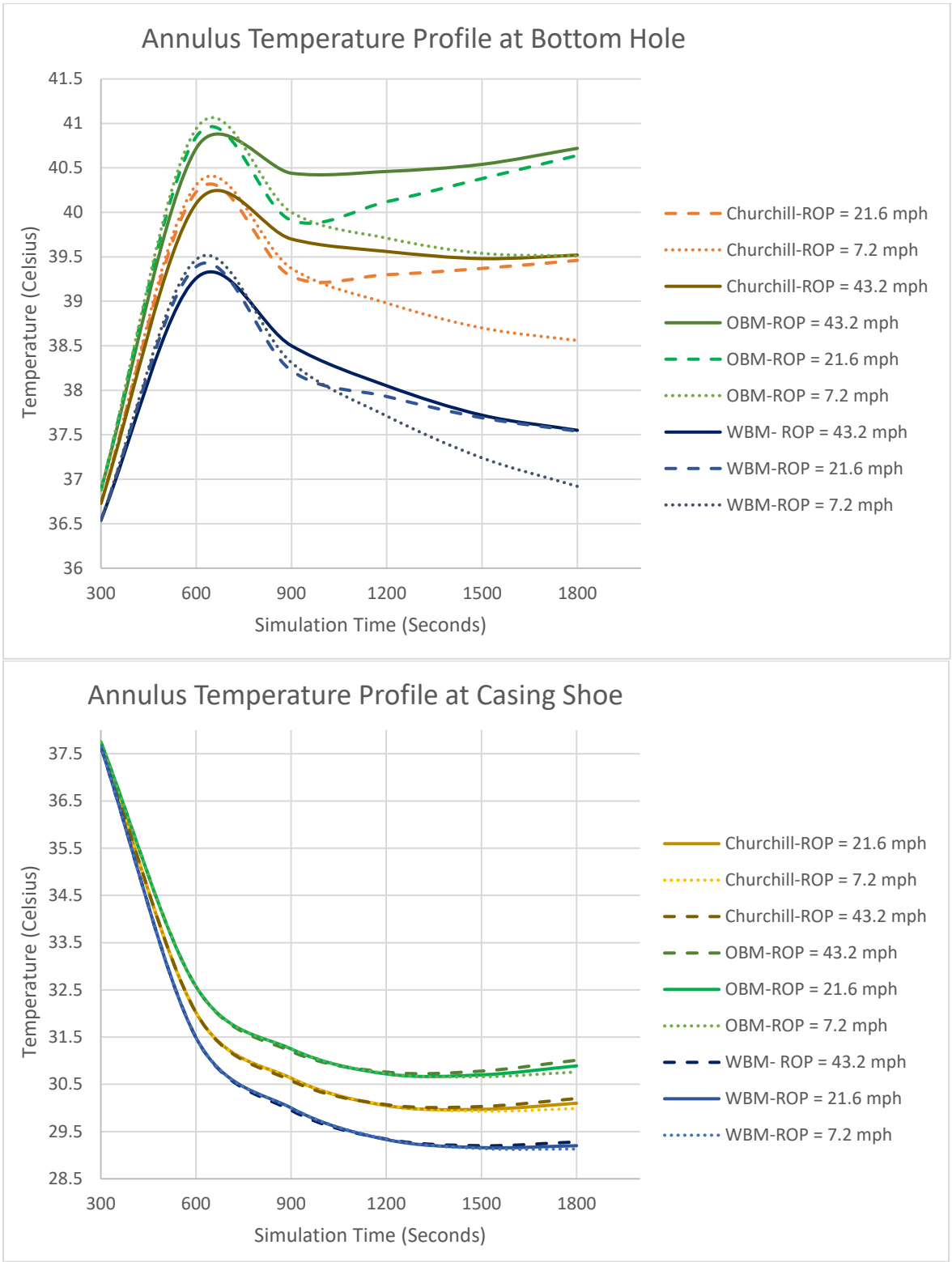

Figure_5.5 Annulus temperature profile at bottom hole and at casing shoe at different ROP

With the start of drilling operation the temperature in the annulus starts to decrease depending upon the rate of penetration but at bottom hole it increases slightly for short time because of heating up of system due to drilling process and then starts to decrease and eventually

become stable. After stabilization, it can be observed that at bottom hole for lower ROP that is 7.2 meters per hour the temperatrure is lower during the drilling process and the temperature is almost same for 21.6 meters per hour and 43.2 meters per hour however at casing shoe the annulus temperature for all different ROP is almost same.

If we compare the different models we can observe that the annulus temperature is maximum for the oil-based mud model and minimum for the water-based mud model because of the higher thermal conductivity and specific heat capacity value of water-based mud than that of oil based mud. At casing shoe, the annulus temperature for OBM based model at the end of drilling process is 30.76°C, for Churchill model it is 30.2°C and for WBM based model the temperature is 29.2°C. The difference in annulus temperature for different ROP values at bottom hole is maximum for OBM based model and minimum for WBM based model.

5.3 Simulation of vertical well

We will now consider the vertical well. Water-based mud of density 1.63 sg with an inlet temperature of 40°C is being used for drilling purpose. Currently well is static and bit depth is 2490 meters while the bottom hole is at 2500 meters. Last casing of 9 5/8- inches is suspended from a depth of 1955 meters and has a casing shoe at 2200 meters.

5.3.1 *Scenario 1*

First scenario is related to flow rate analysis for the three models that is Churchilll model, oil-based mud and water-based mud model. Well was circulated at flow rate of 2500 liters per minute until the temperature stabilized. The summary of simulations performed is given in the table below.

Table_5.5

Simulation	Changing Parameter	Value of Changed Parameter
1	Model	Churchill Model
2	Model	OBM Model
3	Model	WBM Model

Annulus temperature profiles for all the three models are given in figure 5.6. Temperature is plotted against the measured depth at different times. Dotted line indicates the time t1 which

represents the beginning of circulation while the solid line indicates the time t2 which represents the time at the end of circulation process.

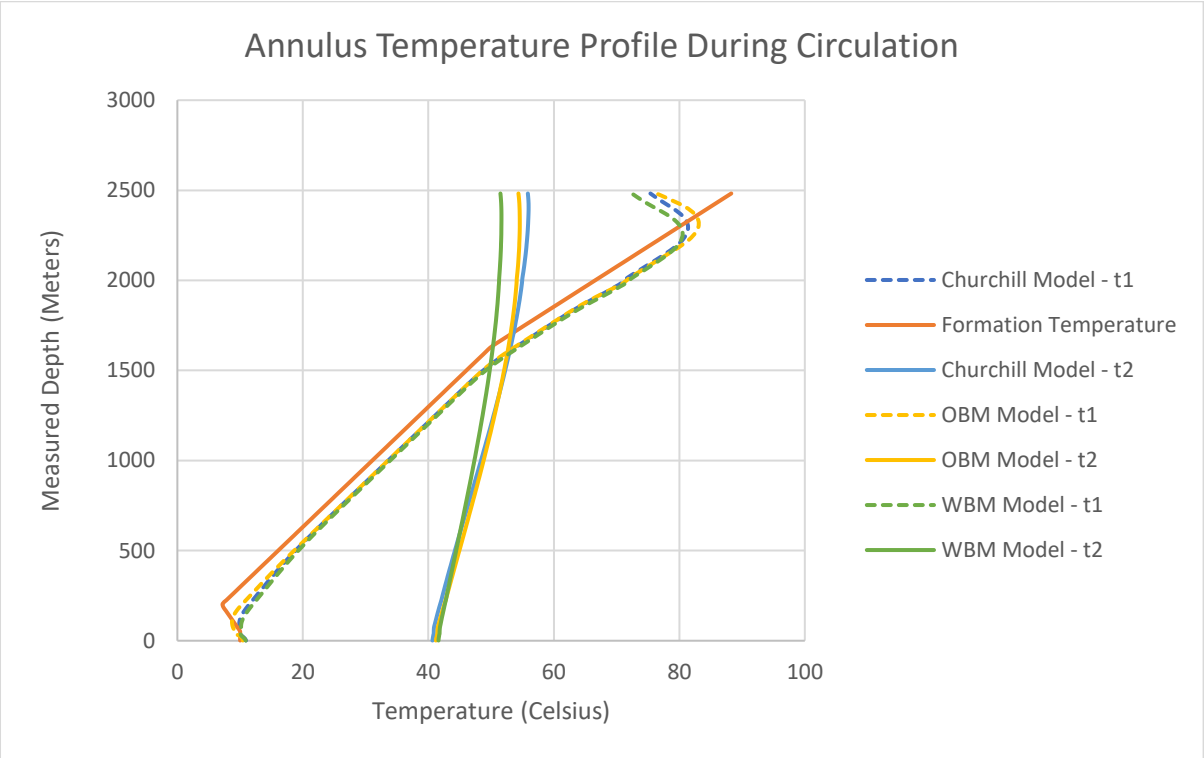

Figure_5.6 Annulus temperature profile during circulation

It can be observed from the figure that all the models follows almost the same trend of temperature variation. At t1 the temperature of annulus is higher and for all the three models it is even higher then the formation temperature but due to circulation the bottom hole temperature starts decreasing. It can be seen that annulus temperature is maximum for Churchill model and minimum for the water-based mud model. Bottom hole temperature for OBM model at the at the end of circulation is 54.36°C. For Churchil model it is 55.86°C and for WBM model the bottom hole temperature is 51.49°C.

5.3.2 *Scenario 2*

Now will do the analysis for rate of penetration for all the three models. For the simulation purpose, well is being drilled at the rate of 28.6 meters per hour. The summary of simulations performed is given in the table below.

Table_5.6

Simulation	Changing Parameter	Value of Changed Parameter

1	Model	OBM model
2	Model	WBM model
3	Model	Churchill model

Bottom hole temperature profile is given below. It can be observed from the figure that all the models follows almost the similar trend of temperature variation while drilling.

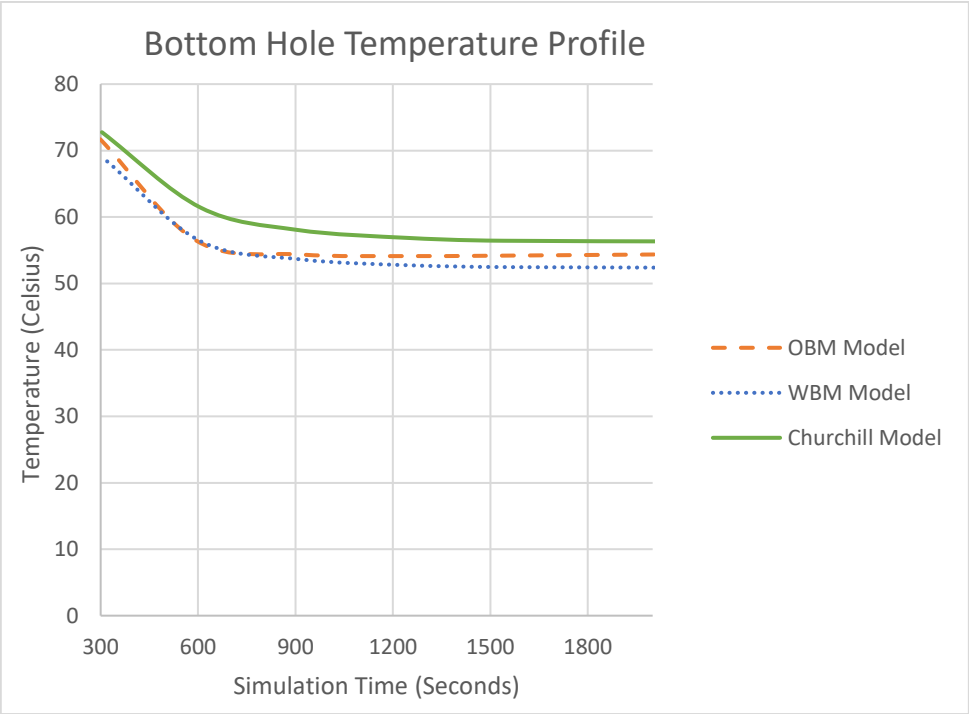

Figure_5.7 Annulus temperature profile at bottom hole during drilling

With the start of drilling operation the temperature in the annulus starts to decrease. There is not much difference in the bottom hole temperature for different models. Bottom hole temperature is maximum for the Churchill model and minimum for the water-based mud model. Bottom hole temperature for OBM model at the at the end of drilling operation is 55.16°C. For Churchil model it is 56.71°C and for WBM model the bottom hole temperature is 52.17°C.

5.4 Conclusion

Results in the chapter 4 proves that our models based on experimental values are more robust and accurate than the models that are being used previously to calculate thermal conductivity and specific heat capacity of the drilling fluid because they consider the chemical change of properties and reaction kinetics of the mixtures as well. Simulation study performed in section 5.2 and 5.3 shows that change in the value of thermal conductivity and specific heat capacity of the drilling fluid affects the temperature distribution along the wellbore. The magnitude of change is an important factor in order to consider the new model. We have considered different scenarios of circulation and drilling for two wells. In horizontal well case, the difference of bottomhole temperature for three models is negligible. During drilling operation the difference in bottom hole temperature between OBM model and Churchill model is 2.65°C while during circulation the difference is 2.55°C. For vertical well case, there is considerable difference of bottomhole temperature for WBM model and the Churchill model. During drilling operation the difference is 5°C while during circulation the difference is 4.5°C. Here, one thing is noted that the magnitude of the change in temperature depends upon the geometry of the wellbore and the simulation time of the drilling or circulation process. Greater is the time of simulation for drilling or circulation process greater difference we have in the temperature profile using our models and the base model.

5.5 Further work recommendations

Simulations of all of the scenarios are performed for a shorter period, it will be interesting to see the trend of temperature evolution while drilling a full section and then circulation.

The instrument used has a limitation for the temperature range when measuring the thermal conductivity of water-based mud. Use of another instrument for experimental purpose can provide further data and also validate the results of our model.

Models presented here are based on unweighted drilling fluid, use of different proportions of sand and weighing material in the drilling mud for experimentation purpose can further improve the model.

REFERENCES

[1] Formate Technical Manual-A7-Thermophysical-Properties. By Cabot, Version 5- 05/16

[2] Adamson, K., Birch, G., Gao, E., Hand, S., Macdonald, C., Mack, D., & Quadri, A. (1998). "High-Pressure, High Temperature Well Construction"

[3] Nave, R. Hyper Physics. "Thermal Conductivity". Georgia State University

[4] NDT Course Material. "Thermal Conductivity". NDT Resource Center.

[5] Sung Hyun Hong and Hae Jin Jo, "Influence of MoS2 Nanosheet Size on Performance of Drilling Mud"

[6] Babak Fazelabdolabadi, Abbas Ali, Khodadadi Mostafa Sedaghatzadeh "Thermal and rheological properties improvement of drilling fluids using functionalized carbon nanotubes"

[7] M. Sedaghatzadeh, A. A. Khodadadi, M. R. Tahmasebi Birgani, "An Improvement in Thermal and Rheological Properties of Water-based Drilling Fluids Using Multiwall Carbon Nanotube (MWCNT)"

[8] https://courses.lumenlearning.com/boundless-physics/chapter/specific-heat/

[9] E. Cayeux, T. Mesagan M. Zidan. "Real time evaluation of hole cleaning conditions with a transient cuttings transport model"

[10] Cornelius B. Bavoha, Titus Ntow Ofeic, Bhajan Lala, "Specific heat capacity of polymer-based drilling fluids: An experimental and correlation study"

[11] http://thermopedia.com/content/1140/

[12] William D. Drotning, Oiega, Peter E. Havey, "Thermal Conductivity of Aqueous Foam"

[13] https://www.nuclear-power.net/nuclear-engineering/heat-transfer/thermal-conduction/thermal-conductivity/thermal-conductivity-of-glass/

[14] Dan Sui, Amare Leulseged, Sima A.Nepal, "kick management study on automated well control for managed pressure drilling in long wells"

[15] EBIKAPAYE, JP, "Effects of Temperature on the Density of Water Based Drilling Mud"

[16] Mou Yang,1 Yingfeng Meng,1 Gao Li, "Estimation of Wellbore and Formation Temperatures during the Drilling Process under Lost Circulation Conditions"

[17] Williams, M. "What is heat conduction?". Phys.Org. December 9, 2014

[18] Mahmood Amani, Mohammed Al-Jubouri “Comparative Study of Using Oil-Based Mud Versus Water-Based Mud in HPHT Fields”

[19] https://opentextbc.ca/physicstestbook2/chapter/temperature-change-and-heat-capacity/

[20] A. García-Gutiérrez, G. Espinosa-Paredes G, Amaro-Espejo “Effect of Variable Rheological Properties of Drilling Muds and Cements on the Temperature Distribution in Geothermal Wells”

[21] M. Kandula “On the Effective Thermal Conductivity of Porous Packed Beds with Uniform Spherical Particles”

[22] Holmes C.S , Swift S.C “Calculation of Circulationg Mud Temperatures, JPT, Vol 22, No. 6,670-674, 1970

[23] Raymond L.R , Swift S.C “Temperature Distribution in a Circulationg Drilling Fluid, JPT, Vol 21. No 3,333-341, 1969

[24] Marshall D.W , Bentsen R.G “A Computer Model to Determine the Temperature Distribution in a Wellbore”

[25] Naziev Ya.M , Gasanov V.G “Determination of Effect of Variability of Thermal Properties of Materials when Measuring Thermal Conductivity Using Steady-State Thermal Methods”

[26] Naziev Ya.M , Gasanov V.G “A Review of Models for Effective Thermal Conductivity of Composite Materials”

APPENDIX

Density measurement is required in order to calculate the specific heat capacity of water-based mud and oil based mud. Density is calculated using Anton Paar density meter and the values are given below:

Temperature	OBM	WBM
20	0.93190	1.08515
30	0.92520	1.08102
40	0.91842	1.07524
50	0.91141	1.06884